NASA Technical Paper 1671

Tire Stiffness and Damping Determined From Static and Free-Vibration Tests

Robert K. Sleeper and Robert C. Dreher

JULY 1980

NASA

NASA Technical Paper 1671

Tire Stiffness and Damping Determined From Static and Free-Vibration Tests

Robert K. Sleeper and Robert C. Dreher
Langley Research Center
Hampton, Virginia

National Aeronautics
and Space Administration

**Scientific and Technical
Information Office**

1980

SUMMARY

Stiffness and damping of a nonrolling tire are determined experimentally from both static force-displacement relations and the free-vibration behavior of a cable-suspended platen pressed against the tire periphery. Lateral and fore-and-aft spring constants and damping factors of a 49 × 17 size aircraft tire for different tire pressures and vertical loads are measured assuming a rate-independent damping form. In addition, a technique is applied for estimating the magnitude of the tire mass which participates in the vibratory motion of the dynamic tests. Results show that both the lateral and fore-and-aft spring constants generally increase with tire pressure but only the latter increased significantly with vertical tire loading. The fore-and-aft spring constants were greater than those in the lateral direction. The static-spring-constant variations were similar to the dynamic variations but exhibited lower magnitudes. Damping was small and insensitive to tire loading. Furthermore, static damping accounted for a significant portion of that found dynamically. Effective tire masses were also small.

INTRODUCTION

Tire stiffness and damping in the lateral and fore-and-aft directions are important properties in dynamic analyses of aircraft wheel shimmy and antiskid braking systems. Static tests on nonrolling tires have been used for a number of years to measure tire stiffness (e.g. ref. 1). Tests on a rolling tire are preferred but equipment and facility limitations make such tests difficult to implement. As a result, tire properties are generally measured using a platen loaded vertically with a tire and supported on bearings (e.g. refs. 2 and 3) where the properties are deduced from the response of the platen to applied forces. Such a support system, however, typically injects indeterminant motion effects and limits tests to static applications. While such static tests remain a primary source of stiffness and damping information, measurements obtained from vibration tests appear to be more representative of the operating environment.

The objective of this report is to discuss the results of an experimental effort to measure stiffness and damping properties of a nonrolling tire using a cable-suspended platen pressed against the tire periphery. Both static and dynamic tests were performed to determine spring constants and damping factors of a large aircraft tire displaced in either the lateral or fore-and-aft direction. Damping is treated in a rate-independent form. Three platens were employed in the dynamic tests to provide an indication of tire mass involvement in the vibratory motion. The study was conducted on a 49 × 17 size tire over a range of vertical loads and inflation pressures extending to their maximum rated values.

SYMBOLS

Values are given in both SI and U.S. Customary Units.

C	damping force coefficient, N-sec/m (lbf-sec/in.)
c.g.	center of gravity
F	complex applied force, N (lbf)
F_{max}	maximum applied force magnitude, N (lbf)
F_o	initial applied force magnitude, N (lbf)
F_v	tire vertical load, N (lbf)
$F_{x=0}$	applied force when displacement is zero, N (lbf)
f	oscillation frequency, Hz
$\underline{i}$	$= \sqrt{-1}$
k	total spring constant, N/m (lbf/in.)
k_c	cable interaction stiffness, N/m (lbf/in.)
k_t	tire spring constant, N/m (lbf/in.)
ℓ	cable length, m (ft)
m	vibrating mass, kg (lbm)
m_p	platen mass, kg (lbm)
m_t	effective tire mass, kg (lbm)
N	number of cycles
t	time, sec
x	complex displacement, m (in.)
x_o	original displacement amplitude, m (in.)
x_N	displacement amplitude of Nth cycle, m (in.)
ζ	viscous damping factor
τ	frequency period, sec
ω	circular forcing frequency, sec^{-1}

APPROACH

Tire spring constants and damping factors in both the lateral and fore-and-aft directions were determined from static and dynamic tests using a cable-suspended platen pressed against the periphery of the tire. Static characteristics were derived from measurements of platen displacement resulting from slowly applied forces. The static spring constant was determined from the slope of the axis of the hysteresis loop described by the force-displacement relationship, and a damping factor was derived from its width. Dynamic characteristics were obtained from simple, single degree of freedom free-vibration tests of the test platen. Thus, for the latter tests the spring constant was derived from the vibrational frequency and platen mass specifications, and the damping factor was determined from the displacement amplitude decay rate. Estimates of the effective tire masses participating in the oscillatory motions of the dynamic tests were determined from changes in the frequency resulting from similar tests with different mass platens.

APPARATUS AND TEST PROCEDURE

Figure 1 is a photograph of the test apparatus and test tire. The apparatus is shown prepared for a lateral dynamic test.

Test Fixture

The main structure of the test fixture is configured as two three-bay portal frames joined overhead by four beams and along the floor by a thick plate. The frames, constructed of welded 10-in. steel H-beams, are nominally 3.0 m (10 ft) deep, 2.2 m (7.1 ft) high and are spaced a distance of 2.1 m (7 ft) apart. The plate along the floor is 2.5 cm (1 in.) thick. The tire rim is supported on the left by a tapered welded box structure, constructed from 2.5-cm (1-in.) thick plate steel, which is suspended from the upper part of the fixture and stabilized by 10.2-cm (4-in.) diameter pipe. A vertical beam also suspended from the upper part of the fixture supports the right side of the rim and clamps it to the fixture to prevent tire rotation.

The special feature of the apparatus is the supporting of the test platen by four cables. Each cable is 1/2-in. steel wire rope and is suspended from a force-measuring load cell connected to a hydraulic cylinder as shown in figure 1. The cable free-swing length ℓ is approximately 1.83 m (6 ft). Tire loading is accomplished by energizing the hydraulic cylinders to lift the platen vertically against the tire; individual cylinder control is available to equalize the cable loading or level the platen.

All test platens were 66 cm (26 in.) square with different thicknesses and material compositions. The two lighter platens were made of aluminum plate. They were 7.6 cm (3 in.) and 13.2 cm (5.19 in.) thick and weighed 102.1 kg (225 lbm) and 173.3 kg (382 lbm), respectively. The heaviest platen was a 15.4-cm (6.06-in.) thick steel plate and weighed 536.1 kg (1182 lbm). The platen test weights included 4.5 kg (10 lbm) for cables and attachments. The upper surface of each platen was painted in the center with a grit-filled enamel to prevent tire slippage.

A separate hydraulic cylinder was used to displace the platen during the static tests. A mechanical ratcheting device and a quick-release mechanism were employed to provide the initial displacement and release for the dynamic tests. The direction of test motion was varied by changing the orientation of the hydraulic cylinder or the displacing mechanism depending on the type of test.

Test Tire

The tests were conducted with a natural rubber, recapped, size 49 × 17, type VII, 26-ply rated aircraft tire of bias-ply construction having a rated inflation pressure of 1220 kPa (177 psi) and a rated maximum vertical load of 178 kN (40 000 lbf). The nominal tire mass was 79.4 kg (175 lbm). The tire was the same tire used in reference 2.

Instrumentation

Cable loads determined from load cells were monitored prior to testing and a linear potentiometer was installed to measure lateral or fore-and-aft displacements during testing. A linear strain gage accelerometer was employed in the dynamic tests to measure platen acceleration. For static testing an additional load cell was utilized to measure external forces that displaced the platen.

Tape recordings of the platen acceleration and displacement were made during the dynamic tests and a time-code generator was incorporated to provide a millisecond time reference.

Test Procedure

After inflating the unloaded tire to the test pressure the platen was prepared for either the static or dynamic tests by centering the platen beneath the tire and uniformly raising it against the tire periphery. Individual hydraulic cylinder adjustments were made to equalize the cable loading and level the platen. In general, vertical loadings were within 3 percent of specified nominal loadings. Platen displacements were kept small to minimize both tire slippage and nonlinear effects.

Static tests.- The static tests were performed by slowly forcing the platen from its neutral position a distance of approximately 0.64 cm (0.25 in.) both laterally and fore and aft through two complete cycles. Corresponding forces and displacements were recorded during the tests which were repeated for each combination of tire pressure, vertical load, and motion direction. For these tests, three tire pressures ranging from 689 (100) to 1241 kPa (180 psi) and the following four vertical loads were examined: 22.2 (5000), 44.5 (10 000), 89.0 (20 000), and 177.9 kN (40 000 lbf).

Dynamic tests.- The dynamic testing was performed by displacing the platen approximately 0.64 cm (0.25 in.), releasing it, and recording the resulting damped free-vibration displacement and acceleration time histories. Tests were conducted for several combinations of platen masses, tire pressures, and vertical loads with both lateral and fore-and-aft motion. Within the dynamic tests the tire was inflated to one of three tire pressures ranging from 689 (100) to 1241 kPa (180 psi) and was subjected to eight vertical loads ranging from 22.2 (5000) to 177.9 kN (40 000 lbf).

DATA REDUCTION AND ANALYSES

The techniques for computing the spring constant and damping factor from the force-displacement relationships of the static tests and the motion of the dynamic tests are given in this section. Also described is the method developed for removing the effect of cable interactions with the computed spring constants. In addition, a technique for computing the effective tire mass from dynamic tests with different mass platens is given.

Spring Constant

Cable interaction.- The following sketch shows the forces acting on the displaced platen and indicates that they are derived from a combination of the

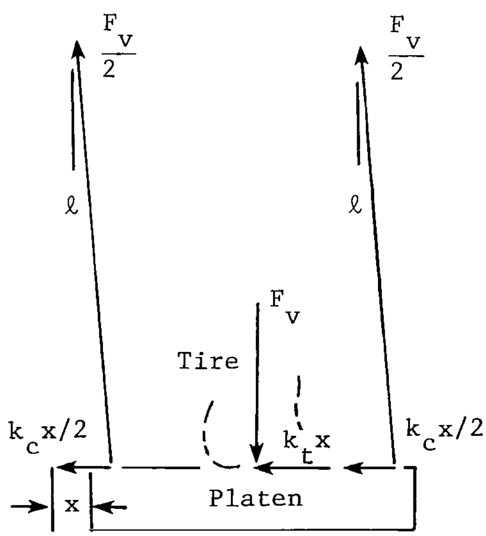

tire stiffness k_t and a component of the cable forces which may be treated as a cable interaction stiffness k_c defined by

$$k_c = \frac{F_v}{\ell}$$

where F_v is the vertical load and ℓ is the free-swing cable length. Thus, the total spring constant k acting on the platen may be resolved into

$$k = k_t + k_c$$

or

$$k_t = k - k_c$$

where the tire spring constants k_t derived from the system must be reduced by the cable interaction stiffness k_c. In this paper it is assumed that cable interaction does not affect the damping or the effective tire mass.

Static tests.- Typical force-displacement curves for both lateral and fore-and-aft tests are presented in figure 2. These hysteresis loops originate at the origin and after two loading cycles terminate at zero load. The load discontinuity at the extreme positions is attributed to tire creep that occurs as the loading directions are manually switched.

For these tests the slope of the force-displacement hysteresis-loop axis (the dashed line connecting the loop extremes) defines the total stiffness applied to the platen. The tire spring constant k_t is found by subtracting the cable interaction stiffness k_c from the total spring constant k.

Dynamic tests.- A typical time history of a dynamic test is displayed in figure 3. The record shows the acceleration and displacement response of the platen to a free-vibration test. Final reference displacement and acceleration levels are indicated along with the displacement envelopes. The analog output of the time-code generator is also shown.

The displacement response exhibited a shift in equilibrium level, attributed to tire creep. Even after accounting for the shift, vibratory periods of the acceleration were more uniform than those of the displacement. Hence, the acceleration time histories, specifically the average of 3 or 4 cycles, were used to compute the vibration frequencies.

For a lightly-damped simple spring-mass system the frequency of vibration is related to the properties of the system by the equation

$$f = \frac{1}{2\pi} \sqrt{k/m} \tag{1a}$$

or

$$\frac{k}{m} = (2\pi f)^2 = \left(\frac{2\pi}{\tau}\right)^2 \tag{1b}$$

where f is the oscillation frequency, τ is the frequency period, and the ratio k/m is termed in this study a frequency parameter. The assumption of small damping is subsequently justified by experiment.

To compute the tire spring constant, the frequency parameter is first determined from the period of vibration and then the total spring constant is computed from the product of the platen mass and the frequency parameter. The spring constant is found by subtracting the cable interaction stiffness from the total spring constant.

Damping Factor

Energy dissipation is manifested in these tests by the hysteretic character of the tire static-force-displacement curves and by the decaying amplitudes of the free-vibration response. To account for this damping in static applications a rate-independent form is required. One such representation called structural damping (e.g. ref. 4) is used in structural vibration analyses (ref. 5). This damping is especially useful for this study in that since damping is small it can readily be related to the more conventional viscous form of damping typically assumed in vibration analyses. Since in free-vibration time histories structural damping is indistinguishable from viscous damping, all damping is treated as structural damping in this paper but expressed in terms of the viscous damping factor.

Static tests.- Light structural damping may be mathematically formulated in terms of the viscous damping factor ζ by the following complex stiffness expression

$$F = (1 + 2\underline{i}\zeta)kx \tag{2}$$

where F is the complex applied force, ζ is the viscous damping factor, k is the conventional (total) spring constant, and x is the complex displacement.

Insight into this force-displacement relationship may be gained by solving for the displacement resulting from the complex sinusoidal force

$$F = F_o e^{\underline{i}\omega t}$$

where F_o is the initial applied force magnitude and ω is the circular forcing frequency. When the force is introduced into the equation the displacement response becomes

$$x = \frac{F_o/k}{1 + 4\zeta^2} e^{\underline{i}(\omega t - 2\zeta)} \tag{3}$$

which when plotted with respect to the applied force yields a tilted ellipse whose width increases with ζ and for small damping the major axis slope approximates the spring constant.

The relationship of the ellipse width to the damping factor ζ may be derived using the real part of the complex applied force and complex displace-ment, i.e.

$$F = F_o \cos \omega t$$

and

$$x = \frac{F_o/k}{1 + 4\zeta^2} \cos (\omega t - 2\zeta)$$

For $x = 0$

$$\omega t = \frac{\pi}{2} + 2\zeta, \quad \frac{3\pi}{2} + 2\zeta, \ \ldots$$

and for small damping at corresponding times the applied force magnitude may be approximated by

$$F_{x=0} = 2F_o\zeta$$

or

$$\zeta = \frac{F_{x=0}}{2F_{max}} \tag{4}$$

Thus, the damping factor for small values is one-half the ratio of the force at zero displacement to the maximum applied force. The following sketch graphically depicts these quantities:

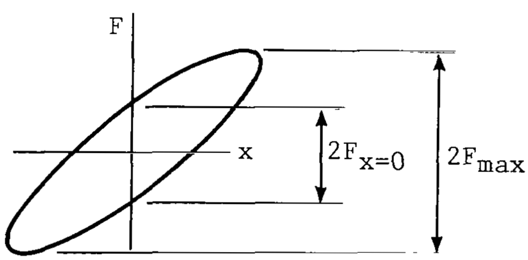

Dynamic tests.- Damping from the dynamic tests was sought from the logarithmic decrement of the decaying displacement amplitude of the free-vibration time history. However, the logarithmic decrement cannot be determined directly from the displacement time history because of its drifting equilibrium level. This nonsymmetry is removed from the displacement data by computing a double amplitude derived from the difference between spline curve-fitted displacement envelopes that pass through the displacement extremes. From the double-amplitude values, damping factors for each test were computed over a few representative cycles using the equation

$$\zeta = \frac{1}{2\pi N} \ln \frac{2x_o}{2x_N} \tag{5}$$

where $2x_N$ is the double amplitude of the Nth cycle and $2x_o$ is the original double amplitude. Should the damping force coefficient C be desired, it may be computed from the following equation:

$$C = 2\zeta \sqrt{k_t m_p} \tag{6}$$

Because of sensor measurement limitations, deflections below 0.25 cm (0.1 in.) were disregarded.

Effective Tire Mass

The solution for the effective tire mass assumes that the mass m of the vibrating body of equation (1) is composed of the platen mass m_p and the effective tire mass m_t, that is

$$m = m_p + m_t \tag{7}$$

By replacing the vibrating mass with the product of the total spring constant and the reciprocal of the frequency parameter, the following relation may be derived:

$$m_p = k\left(\frac{m}{k}\right) - m_t \tag{8}$$

The effective tire mass is then found from a coefficient obtained from a linear regression analysis of equation (8).

RESULTS AND DISCUSSION

Static and dynamic tests were conducted in the lateral and fore-and-aft directions to determine tire spring constants and damping factors. Dynamic tests with different mass platens provided insight into the amount of tire mass participating in the dynamic motion. In the following sections dynamic results are discussed and static results are presented for comparison. To confirm that the cable-suspended system exhibited no significant coupling between the pitching and translating motions of its platen, a two-degree-of-freedom analysis of these platen motions is presented in the appendix.

Summaries of the test conditions and results for the lateral and fore-and-aft free-vibration tests are given in tables I and II. Test conditions and results for the static tests are given in table III. As shown in the tables, lateral and fore-and-aft dynamic tests were conducted using three platens ranging in mass from 102 (225) to 536 kg (1182 lbm). The tire was inflated to one of three pressures ranging from 689 (100) to 1241 kPa (180 psi) where the rated inflation pressure was 1220 kPa (177 psi). The tire was also loaded with one of eight (nominal) vertical loads ranging from 22.2 kN (5000 lbf) to the rated maximum load of 177.9 kN (40 000 lbf).

One of the reasons for employing small amplitudes in the tests is to minimize nonlinearities that can occur for systems undergoing large deflections. Some insight into the extent of this type of nonlinearity can be gained from the data. The dynamic tests revealed a slight frequency increase with amplitude decay. This nonlinear effect, however, was deemed insignificant since no curvature of the spine of the static hysteresis loop was apparent (e.g. fig. 2). Thus, when frequency variations occurred during a test, they were averaged. The determination of spring constants, damping factors, and effective tire masses is discussed in the sections that follow.

Spring Constants

Lateral and fore-and-aft frequency parameters derived from the oscillation periods of the acceleration time histories for each platen mass, tire pressure, and nominal vertical load are tabulated in tables I and II, respectively. Spring constants computed from frequency parameters and their platen mass are also given in the tables. Spring constants determined statically are given in table III.

Lateral direction.- The lateral-frequency-parameter values derived from vibration periods using equation (1) are displayed in figure 4. As expected, the lateral frequency parameter decreases with increasing platen mass. For each platen mass the frequency parameter increases with inflation pressure. The tire lateral spring constants computed from these data, and listed in table I, are noted to be essentially insensitive to platen mass. Thus, the dynamic lateral spring constants presented in figure 5(a) as a function of vertical load were obtained for each pressure and loading condition by averaging the data obtained for each platen. The averaged dynamic lateral spring constants which range from 937 (5350) to 1471 kN/m (8400 lbf/in.), for the test conditions described in this paper, are shown to increase with inflation pressure. When the pressure is held constant the spring constants reach a maximum value at some intermediate vertical loading.

The spring constants obtained from static tests are presented in figure 5(b). The static values are shown to exhibit trends similar to the dynamic values for equivalent test conditions, but are 10 to 20 percent lower than those found in the dynamic tests.

For purposes of comparing these data with those from other sources, spring constants are displayed as functions of tire vertical deflection in figure 6. The vertical tire deflections are listed in table IV. Data trends in figure 6 are similar to those of reference 1; however, the linear empirical equation of the reference does not describe these trends in the low deflection range of the study.

Fore-and-aft direction.- The dynamic fore-and-aft frequency parameters are displayed in figure 7 and, as expected, the frequency parameter is shown to increase with decreasing platen mass. In general, the fore-and-aft frequency parameter is less sensitive to variations in inflation pressure and more sensitive to variations in the vertical load than the lateral frequency parameters. Since the tire fore-and-aft spring constants computed from these data were also found to be essentially insensitive to platen mass (see table II), the dynamic spring constants for the three platens were averaged for each pressure and loading condition (fig. 8(a)).

The averaged dynamic fore-and-aft tire-spring-constant values range from 2014 (11 500) to 3677 kN/m (21 000 lbf/in.) and are considerably larger than the lateral-spring-constant values for comparable test conditions. The data of figure 8(a) show that these spring constants increase with inflation pressure at the higher vertical loads and generally increase with vertical load when the inflation pressure is held constant.

The static fore-and-aft spring-constant values, which are presented as a function of vertical load in figure 8(b), show trends similar to the dynamic data. However, the static-spring-constant values are 20 to 35 percent less than the dynamic values. This reduction is attributed, in part, to the viscoelastic nature of the tire.

Fore-and-aft tire spring constants are presented as a function of tire vertical deflection in figure 9. Data from both the dynamic tests (fig. 9(a)) and the static tests (fig. 9(b)) indicate that the fore-and-aft tire spring constant generally increases with vertical deflections.

Reference 3 contains lateral static spring constants measured from the same type of tire used in this report, and reference 2 contains fore-and-aft static-spring-constant data from the same tire used in this report. The scant data from the references indicate similar trends but the stiffness values from both sets of data were below the static values of this study. One cause for these differences may be that the test amplitudes of this study were appreciably lower than those of references 2 and 3. As mentioned in reference 1, spring constants increase with reduced test amplitude. Other causes may be due to tire age, material, and construction inconsistencies that may occur in the same tire as well as in different tires of the same size.

Damping Factor

Lateral and fore-and-aft damping factors derived from the displacement amplitudes of the damped free vibration of each test are tabulated in tables I and II, respectively. Damping factors determined from static tests are given in table III.

Lateral direction.- The damping factors derived from vibratory motion in the lateral direction, presented in figure 10(a), are small and range from 2 to 7 percent of critical damping. The dynamic lateral damping factors generally appear to be insensitive to vertical load variations and no consistent trends are noted with variations in tire inflation pressure. The data do indicate a tendency for the lateral damping factors to decrease with increasing platen mass.

The lateral damping factors obtained from the static tests are presented in figure 10(b) and are approximately equal in magnitude to the dynamic-damping-factor values of the heavy weight platen. These results would indicate that the increased dynamic damping factors associated with the two lighter platens may be the result of some additional viscous damping.

Fore-and-aft direction.- The damping factors derived from the fore-and-aft tests are shown in figure 11. The dynamic fore-and-aft damping factors (fig. 11(a)) range between approximately 4 and 9 percent of critical damping and no consistent trends are observed with variations in the test conditions.

The fore-and-aft damping factors obtained from the static tests are presented in figure 11(b) and are noted to be consistently lower than the dynamic damping factors, thereby indicating that some viscous damping is present during fore-and-aft tire vibrations. A comparison of the static damping factors from the lateral tests and the fore-and-aft tests indicate slightly higher damping in the fore-and-aft directions.

The findings from the damping tests in both directions indicate that damping was sufficiently small to justify the deletion of damping effects in the stiffness computations.

Effective Tire Mass

Effective tire masses are computed from the lateral and fore-and-aft dynamic tests for each tire pressure and vertical load combination.

Lateral direction.- The effective tire mass in the lateral direction was computed using all three different mass platens and is given in table I for each tire pressure and loading condition.

The results are shown to vary from 2.7 (6.0) to 13.9 kg (30.7 lbm) and have an average value of 7.5 kg (16.5 lbm). When compared to the total tire mass of 79.4 kg (175 lbm) the average effective tire mass is small. One reason for the variations in the effective-tire-mass data is attributed to a lack of instrumentation precision as illustrated in the following error analysis.

The mass error Δm occurring from a period inaccuracy $\Delta\tau$ can be derived from equation (1) to be

$$\Delta m = \frac{m_p \sqrt{k/m}}{\pi} \Delta\tau \qquad (9)$$

Thus, for a period inaccuracy of 1 msec, the equation indicates that Δm will be within the following range:

$$3.0 \text{ kg } (6.6 \text{ lbm}) < \Delta m < 9.1 \text{ kg } (20.1 \text{ lbm})$$

Fore-and-aft direction.- Upon examination of the fore-and-aft data, the spring constants for the heavy platen were found to be changing with frequency; hence, no effective tire mass was computed for that platen in the fore-and-aft direction. The effective tire masses associated with the test data from the remaining two platens are given in table II. These masses were generally higher than those associated with the lateral tests and ranged from 7.8 (17.2) to 25.9 kg (57.2 lbm) with an average value of 15.6 kg (34.4 lbm). Equation (9) predicts mass errors in the range of

$$4.45 \text{ kg } (9.8 \text{ lbm}) < \Delta m < 8.3 \text{ kg } (18.2 \text{ lbm})$$

for a period inaccuracy of 1 msec.

The analysis of both the lateral and fore-and-aft test series indicates that better instrumentation or more sophisticated data reduction techniques are needed to accurately define the effective tire mass. However, these results do indicate that the effective tire mass associated with vibratory motion is only a small fraction of the total tire mass.

CONCLUDING REMARKS

Lateral and fore-and-aft stiffness and damping of a nonrolling tire were measured using a cable-suspended platen pressed against the tire periphery. Tire properties were determined from the platen free-vibration or dynamic behavior as well as from static force-displacement tests. The effective tire mass participating in the free-vibration motion was also estimated.

By using this method, lateral and fore-and-aft properties were determined for a 49 × 17, type VII, 26-ply rated aircraft tire of bias-ply design. The results showed the following:

1. Lateral spring constants varied little with vertical load but increased significantly with tire pressure.

2. Fore-and-aft spring constants increased significantly with vertical load and, except for low vertical loads, also with tire pressure.

3. Fore-and-aft spring constants were greater than lateral spring constants.

4. Static-spring-constant variations exhibited trends similar to those found dynamically but were 10 to 20 percent less in the lateral direction and 20 to 35 percent less in the fore-and-aft direction.

5. Damping in both the lateral and fore-and-aft directions was less than 10 percent of critical damping and insensitive to vertical loads. Static damping was lower than dynamic damping but was a significant portion of the damping at lower frequencies.

6. Effective tire mass was difficult to determine accurately because of insufficient instrumentation resolution, but the results of this investigation indicated that it was a small fraction of the total tire mass.

The results of this study indicate that this method of tire analysis is suitable for establishing static and dynamic tire stiffness magnitudes, trends, and ranges of tire damping. It may also be useful in estimating effective tire mass.

Langley Research Center
National Aeronautics and Space Administration
Hampton, VA 23665
May 5, 1980

APPENDIX

PITCH AND TRANSLATIONAL MOTION ANALYSIS OF TEST APPARATUS

In the analysis of this report it is convenient to derive the total spring constant k from the simplest form of the undamped natural frequency relationship $f = \frac{\sqrt{k/m}}{2\pi}$. However, because the constraining action of the tire and cables acts above the platen c.g. the pitch and translational motion of the platen could couple and the frequency deviate from the simply determined value.

To show the effect of these conditions, equations of motion are presented for the translational and pitch degrees of freedom of the test apparatus, and the attendant natural frequencies are analyzed. Effects of parametric motion of the cables are ignored. The tire and platen are represented schematically in the following figure:

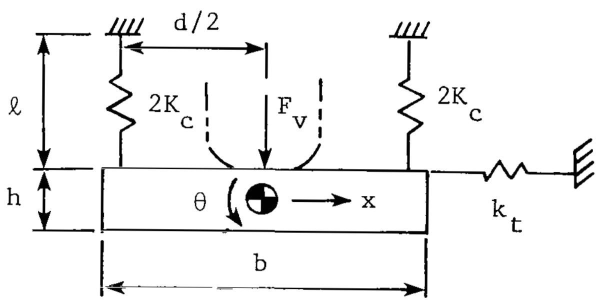

Let

b	base width of platen mass
d	width between cables
F_v	tire vertical load
f	oscillation frequency
h	platen thickness
K_c	extensional cable stiffness
k	total spring constant
k_t	tire spring constant
ℓ	cable length

APPENDIX

m	platen mass
J	platen polar moment of inertia
x	platen lateral displacement
θ	platen pitch attitude
ω	circular forcing frequency

Dots over a symbol indicate a derivative with respect to time.

$$m\ddot{x} = -k_t\left(x - \frac{h}{2}\theta\right) - \frac{F_v}{\ell}x \tag{A1}$$

$$J\ddot{\theta} = -d^2K_c\theta + k_t\frac{h}{2}\left(x - \frac{h}{2}\theta\right) + \frac{hF_v}{2\ell}x \tag{A2}$$

where

$$J = \frac{m(b^2 + h^2)}{12}$$

For harmonic motion of frequency ω, the two equations yield

$$\omega^4 - \left[\frac{1}{m}\left(k_t + \frac{F_v}{\ell}\right) + \frac{1}{J}\left(d^2K_c + \frac{h^2k_t}{4}\right)\right]\omega^2 + \frac{d^2K_c\left(k_t + \frac{F_v}{\ell}\right)}{mJ} = 0 \tag{A3}$$

If the platen thickness h approaches zero, no coupling exists and equation (A3) yields

$$\omega_1{}^2 = \frac{1}{m}\left(k_t + \frac{F_v}{\ell}\right) \tag{A4}$$

and

$$\omega_2{}^2 = \frac{d^2K_c}{J} \tag{A5}$$

where ω_1 is the uncoupled translational frequency of the platen and ω_2 the pitching frequency. Even the uncoupled translational frequency is shown to differ from the simple form of the frequency relation by a pendulum effect.

APPENDIX

For the parameter values of table A1 the uncoupled frequencies are

$$\omega_1 = \left(\frac{k_t}{m} + \frac{F_v}{m\ell}\right)^{1/2} = (18\ 188 + 350)^{1/2} = 136.1 \text{ rad/sec}$$

and

$$\omega_2 = \left(\frac{d^2 K_c}{J}\right)^{1/2} = 918.5 \text{ rad/sec}$$

where

$$(k_t/m)^{1/2} = 134.9 \text{ rad/sec}$$

These results indicate the negligible amount of translational stiffening attributed to the suspension system (about 1 percent) and show a large frequency separation between the two modes.

For the same parameter values the coupled equations yield

$$\omega_1 = 136.0 \text{ rad/sec}$$

and

$$\omega_2 = 919.7 \text{ rad/sec}$$

which differ only slightly from the uncoupled values.

Thus, little stiffness computation error can be expected from usage of the simple frequency expression $f = \frac{\sqrt{k/m}}{2\pi}$.

TABLE A1.- VALUES OF PARAMETERS USED IN ANALYSIS OF TEST APPARATUS

Parameter	SI Units	U.S. Customary Units
b	66.0 cm	26 in.
d	61.0 cm	24 in.
F_v	177.9 kN	40 000 lbf
h	13.2 cm	5.19 in.
K_c	14 870 kN/m	84 910 lbf/in.
k_t	3152 kN/m	18 000 lbf/in.
ℓ	293.6 cm	115.6 in.
m	173 kg	382 lbm

REFERENCES

1. Smiley, Robert F.; and Horne, Walter B.: Mechanical Properties of Pneumatic Tires With Special Reference to Modern Aircraft Tires. NASA TR R-64, 1960. (Supersedes NACA TN 4110.)

2. Tanner, John A.; McCarty, John L.; and Batterson, Sidney A.: The Elastic Response of Bias-Ply Aircraft Tires to Braking Forces. NASA TN D-6426, 1971.

3. Collins, R. L.; and Black, R. J.: Tire Parameters for Landing-Gear Shimmy Studies. J. Aircr., vol. 6, no. 3, May-June 1969, pp. 252-258.

4. Scanlan, Robert H.; and Rosenbaum, Robert: Introduction to the Study of Aircraft Vibration and Flutter. Macmillan Co., c.1951.

5. Hurty, Walter C.; and Rubinstein, Moshe F.: Dynamics of Structures. Prentice-Hall, Inc., c.1964.

TABLE I. - SUMMARY OF LATERAL DYNAMIC TEST CONDITIONS AND RESULTS

Test	Platen mass		Tire pressure		Nominal vertical load		Frequency parameter	Spring constant		Damping factor	Effective tire mass	
	kg	lbm	kPa	psi	kN	lbf	$1/sec^2$	kN/m	lbf/in.		kg	lbm
1	102	225	689	100	22.2	5 000	8 506	856	4888	0.055	13.9	30.7
2					44.5	10 000	9 601	956	5457	.053	11.3	24.9
3					66.7	15 000	10 523	1038	5926	.061	7.8	17.2
4					89.0	20 000	10 480	1021	5831	.061	6.5	14.3
5					111.2	25 000	9 986	959	5474	.060	-	-
6					133.4	30 000	9 676	915	5224	.059	5.4	11.9
7					155.7	35 000	9 563	891	5088	.059	6.1	13.5
8					177.9	40 000	-	-	-	-	-	-
9			965	140	22.2	5 000	10 215	1030	5884	.060	3.2	7.0
10					44.5	10 000	11 735	1173	6701	.061	4.3	9.6
11					66.7	15 000	12 367	1226	7001	.062	3.2	7.1
12					89.0	20 000	12 151	1191	6805	.063	8.5	18.8
13					111.2	25 000	11 982	1162	6637	.064	4.8	10.7
14					133.4	30 000	11 635	1115	6366	.066	10.3	22.8
15					155.7	35 000	11 470	1086	6200	.062	8.0	17.6
16					177.9	40 000	11 089	1035	5909	.060	13.7	30.2
17			1241	180	22.2	5 000	10 830	1093	6242	.058	-	-
18					44.5	10 000	12 653	1267	7236	.047	2.7	6.0
19					66.7	15 000	13 610	1353	7725	.050	4.5	10.0
20					89.0	20 000	14 215	1402	8008	.051	7.7	16.9
21					111.2	25 000	14 269	1396	7970	.051	7.3	16.1
22					133.4	30 000	14 269	1384	7901	.053	11.2	24.7
23					155.7	35 000	14 121	1356	7745	.055	8.9	19.7
24					177.9	40 000	13 793	1311	7485	.047	7.4	16.3
25	173	382	689	100	22.2	5 000	5 516	944	5389	0.034	13.9	30.7
26					44.5	10 000	6 036	1026	5861	.031	11.3	24.9
27					66.7	15 000	6 184	1035	5912	.029	7.8	17.2
28					89.0	20 000	5 914	976	5575	.030	6.5	14.3
29					111.2	25 000	-	-	-	-	-	-
30					133.4	30 000	5 696	914	5221	.032	5.4	11.9
31					155.7	35 000	5 676	899	5131	.032	6.1	13.5
32					177.9	40 000	5 679	887	5065	.033	-	-
33			965	140	22.2	5 000	6 207	1063	6073	.043	3.2	7.0
34					44.5	10 000	6 903	1172	6692	.038	4.3	9.6
35					66.7	15 000	7 476	1259	7191	.040	3.2	7.1
36					89.0	20 000	7 408	1235	7053	.036	8.5	18.8
37					111.2	25 000	7 510	1241	7085	.039	4.8	10.7
38					133.4	30 000	7 209	1176	6718	.038	10.3	22.8
39					155.7	35 000	7 113	1148	6553	.038	8.0	17.6
40					177.9	40 000	6 845	1098	6269	.037	13.7	30.2
41			1241	180	22.2	5 000	6 286	1077	6150	.051	-	-
42					44.5	10 000	7 283	1238	7068	.043	2.7	6.0
43					66.7	15 000	7 831	1321	7542	.047	4.5	10.0
44					89.0	20 000	7 971	1333	7610	.045	7.7	16.9
45					111.2	25 000	8 173	1356	7741	.045	7.3	16.1
46					133.4	30 000	8 232	1354	7730	.047	11.2	24.7
47					155.7	35 000	8 080	1315	7510	.044	8.9	19.7
48					177.9	40 000	8 212	1326	7571	.046	7.4	16.3

TABLE I. - Concluded

Test	Platen mass		Tire pressure		Nominal vertical load		Frequency parameter	Spring constant		Damping factor	Effective tire mass	
	kg	lbm	kPa	psi	kN	lbf	1/sec^2	kN/m	lbf/in.		kg	lbm
49	536	1182	689	100	22.2	5 000	1839	974	5561	0.037	13.9	30.7
50					44.5	10 000	2014	1056	6028	.031	11.3	24.9
51					66.7	15 000	2088	1083	6186	.029	7.8	17.2
52					89.0	20 000	2019	1034	5904	.030	6.5	14.3
53					111.2	25 000	-	-	-	-	-	-
54					133.4	30 000	1897	944	5393	.033	5.4	11.9
55					155.7	35 000	1891	929	5304	.033	6.1	13.5
56					177.9	40 000	1907	925	5284	.034	-	-
57			965	140	22.2	5 000	2014	1068	6097	.040	3.2	7.0
58					44.5	10 000	2287	1202	6864	.032	4.3	9.6
59					66.7	15 000	2432	1268	7239	.028	3.2	7.1
60					89.0	20 000	2470	1276	7286	.026	8.5	18.8
61					111.2	25 000	2426	1240	7082	.027	4.8	10.7
62					133.4	30 000	2409	1219	6961	.028	10.3	22.8
63					155.7	35 000	2347	1173	6701	.028	8.0	17.6
64					177.9	40 000	2340	1156	6610	.029	13.7	30.2
65			1241	180	22.2	5 000	-	-	-	-	-	-
66					44.5	10 000	2414	1270	7253	.033	2.7	6.0
67					66.7	15 000	2622	1370	7821	.028	4.5	10.0
68					89.0	20 000	2746	1424	8131	.027	7.7	16.9
69					111.2	25 000	2784	1432	8178	.024	7.3	16.1
70					133.4	30 000	2853	1457	8320	.023	11.2	24.7
71					155.7	35 000	2777	1404	8017	.024	8.9	19.7
72					177.9	40 000	2751	1378	7869	.026	7.4	16.3

TABLE II. - SUMMARY OF FORE-AND-AFT DYNAMIC TEST CONDITIONS AND RESULTS

Test	Platen mass		Tire pressure		Nominal vertical load		Frequency parameter	Spring constant		Damping factor	Effective tire mass	
	kg	lbm	kPa	psi	kN	lbf	1/sec^2	kN/m	lbf/in.		kg	lbm
73	102	225	689	100	22.2	5 000	20 863	2117	12 091	-	-	-
74					44.5	10 000	25 090	2537	14 486	0.055	9.8	21.5
75					66.7	15 000	27 340	2754	15 729	.053	14.2	31.4
76					89.0	20 000	27 340	2742	15 659	.056	22.1	48.8
77					111.2	25 000	27 826	2780	15 873	.058	22.1	48.7
78					133.4	30 000	28 325	2819	16 095	.058	18.0	39.6
79					155.7	35 000	29 364	2912	16 630	.060	13.4	29.5
80					177.9	40 000	30 462	3012	17 201	.060	20.7	45.7
81			965	140	22.2	5 000	20 392	2069	11 816	-	-	-
82					44.5	10 000	-	-	-	-	-	-
83					66.7	15 000	28 837	2907	16 601	.062	7.8	17.3
84					89.0	20 000	30 746	3090	17 644	.072	16.0	35.2
85					111.2	25 000	31 326	3137	17 913	.060	15.3	33.7
86					133.4	30 000	31 772	3170	18 104	.061	10.6	24.3
87					155.7	35 000	31 772	3158	18 034	.063	15.5	34.2
88					177.9	40 000	31 622	3131	17 878	.060	17.0	37.5
89			1241	180	22.2	5 000	18 657	1892	10 805	-	18.7	41.2
90					44.5	10 000	24 881	2515	14 364	.052	9.3	20.6
91					66.7	15 000	28 837	2907	16 601	.053	7.8	17.2
92					89.0	20 000	30 889	3104	17 727	.061	12.8	28.3
93					111.2	25 000	32 850	3292	18 801	.073	21.9	48.3
94					133.4	30 000	34 830	3482	19 886	.068	16.4	36.2
95					155.7	35 000	34 830	3470	19 816	.072	25.9	57.2
96					177.9	40 000	35 530	3530	20 155	.071	11.7	25.9
97	173	382	689	100	22.2	5 000	12 151	2094	11 955	0.086	-	-
98					44.5	10 000	15 328	2632	15 030	.057	9.8	21.5
99					66.7	15 000	16 958	2902	16 574	.049	14.2	31.4
100					89.0	20 000	17 375	2962	16 917	.067	22.1	48.8
101					111.2	25 000	17 683	3004	17 153	.051	22.1	48.7
102					133.4	30 000	17 777	3008	17 177	.048	18.0	39.6
103					155.7	35 000	18 160	3062	17 486	.060	13.4	29.5
104					177.9	40 000	19 281	3244	18 526	.051	20.7	45.7
105			965	140	22.2	5 000	11 803	2033	11 611	.094	-	-
106					44.5	10 000	15 328	2632	15 030	.058	-	-
107					66.7	15 000	17 497	2996	17 108	.054	7.8	17.3
108					89.0	20 000	19 175	3274	18 698	.047	16.0	35.2
109					111.2	25 000	19 496	3318	18 947	.050	15.3	33.7
110					133.4	30 000	19 496	3306	18 878	.054	10.6	24.3
111					155.7	35 000	19 788	3344	19 097	.057	15.5	34.2
112					177.9	40 000	19 788	3332	19 028	.060	17.0	37.5
113			1241	180	22.2	5 000	11 735	2021	11 543	.091	18.7	41.2
114					44.5	10 000	15 178	2606	14 882	.060	9.3	20.6
115					66.7	15 000	17 497	2996	17 107	.052	7.8	17.2
116					89.0	20 000	19 069	3256	18 593	.046	12.8	28.3
117					111.2	25 000	20 863	3555	20 300	.051	21.9	48.3
118					133.4	30 000	21 754	3697	21 112	.044	16.4	36.2
119					155.7	35 000	22 380	3793	21 662	.051	25.9	57.2
120					177.9	40 000	21 857	3691	21 075	.057	11.7	25.9

TABLE II. - Concluded

Test	Platen mass		Tire pressure		Nominal vertical load		Frequency parameter	Spring constant		Damping factor	Effective tire mass	
	kg	lbm	kPa	psi	kN	lbf	$1/sec^2$	kN/m	lbf/in.		kg	lbm
121	536	1182	689	100	22.2	5 000	3 889	2073	11 839	0.062		
122					44.5	10 000	4 807	2553	14 581	.058		
123					66.7	15 000	5 338	2826	16 138	.057		
124					89.0	20 000	5 513	2907	16 604	.057		
125					111.2	25 000	5 551	2916	16 651	.058		
126					133.4	30 000	5 685	2976	16 992	.057		
127					155.7	35 000	5 748	2997	17 115	.061		
128					177.9	40 000	6 092	3170	18 100	.059		
129			965	140	22.2	5 000	3 782	2016	11 511	.066		
130					44.5	10 000	4 794	2546	14 541	.057		
131					66.7	15 000	5 496	2911	16 622	.051		
132					89.0	20 000	5 962	3148	17 979	.050		
133					111.2	25 000	6 169	3247	18 543	.052		
134					133.4	30 000	6 227	3266	18 652	.055		
135					155.7	35 000	6 149	3212	18 343	.057		
136					177.9	40 000	6 207	3231	18 452	.052		
137			1241	180	22.2	5 000	3 948	2105	12 019	.069		
138					44.5	10 000	4 741	2518	14 379	.057		
139					66.7	15 000	5 464	2894	16 524	.052		
140					89.0	20 000	5 907	3119	17 810	.050		
141					111.2	25 000	6 366	3353	19 147	.048		
142					133.4	30 000	6 531	3429	19 583	.049		
143					155.7	35 000	6 658	3485	19 902	.048		
144					177.9	40 000	6 724	3508	20 035	.057		

TABLE III. - SUMMARY OF STATIC TEST CONDITIONS AND RESULTS

Test	Tire pressure		Nominal vertical load		Spring constant		Damping factor
	kPa	psi	kN	lbf	kN/m	lbf/in.	
Lateral							
1	689	100	22.2	5 000	831	4 748	0.035
2			44.5	10 000	930	5 309	.033
3			89.0	20 000	919	5 248	.032
4			177.9	40 000	826	4 717	.031
5	965	140	22.2	5 000	895	5 113	.041
6			44.5	10 000	1055	6 025	.038
7			89.0	20 000	1127	6 436	.033
8			177.9	40 000	966	5 517	.036
9	1241	180	22.2	5 000	914	5 217	.032
10			44.5	10 000	1086	6 200	.033
11			89.0	20 000	1265	7 226	.030
12			177.9	40 000	1210	6 911	.029
Fore and aft							
13	689	100	22.2	5 000	1632	9 321	0.050
14			44.5	10 000	2042	11 663	.039
15			89.0	20 000	2289	13 074	.039
16			177.9	40 000	2598	14 834	.041
17	965	140	22.2	5 000	1460	8 335	.051
18			44.5	10 000	1949	11 129	.041
19			89.0	20 000	2413	13 780	.039
20			177.9	40 000	2636	15 052	.039
21	1241	180	22.2	5 000	1442	8 234	.048
22			44.5	10 000	1951	11 139	.047
23			89.0	20 000	2583	14 748	.037
24			177.9	40 000	2913	16 632	.039

TABLE IV. - VALUES OF VERTICAL TIRE DEFLECTION

Tire pressure		Vertical load		Vertical tire deflection	
kPa	psi	kN	lbf	cm	in.
689	100	22.2	5 000	2.39	0.94
		44.5	10 000	4.24	1.67
		66.7	15 000	5.84	2.30
		89.0	20 000	7.24	2.85
		111.2	25 000	8.56	3.37
		133.4	30 000	9.90	3.90
		155.7	35 000	11.30	4.45
		177.9	40 000	12.65	4.98
965	140	22.2	5 000	1.90	.75
		44.5	10 000	3.35	1.32
		66.7	15 000	4.67	1.84
		89.0	20 000	5.84	2.30
		111.2	25 000	6.91	2.72
		133.4	30 000	7.92	3.12
		155.7	35 000	8.89	3.50
		177.9	40 000	9.83	3.87
1241	180	22.2	5 000	1.75	.69
		44.5	10 000	3.17	1.25
		66.7	15 000	4.37	1.72
		89.0	20 000	5.41	2.13
		111.2	25 000	6.30	2.48
		133.4	30 000	7.14	2.81
		155.7	35 000	7.95	3.13
		177.9	40 000	8.74	3.44

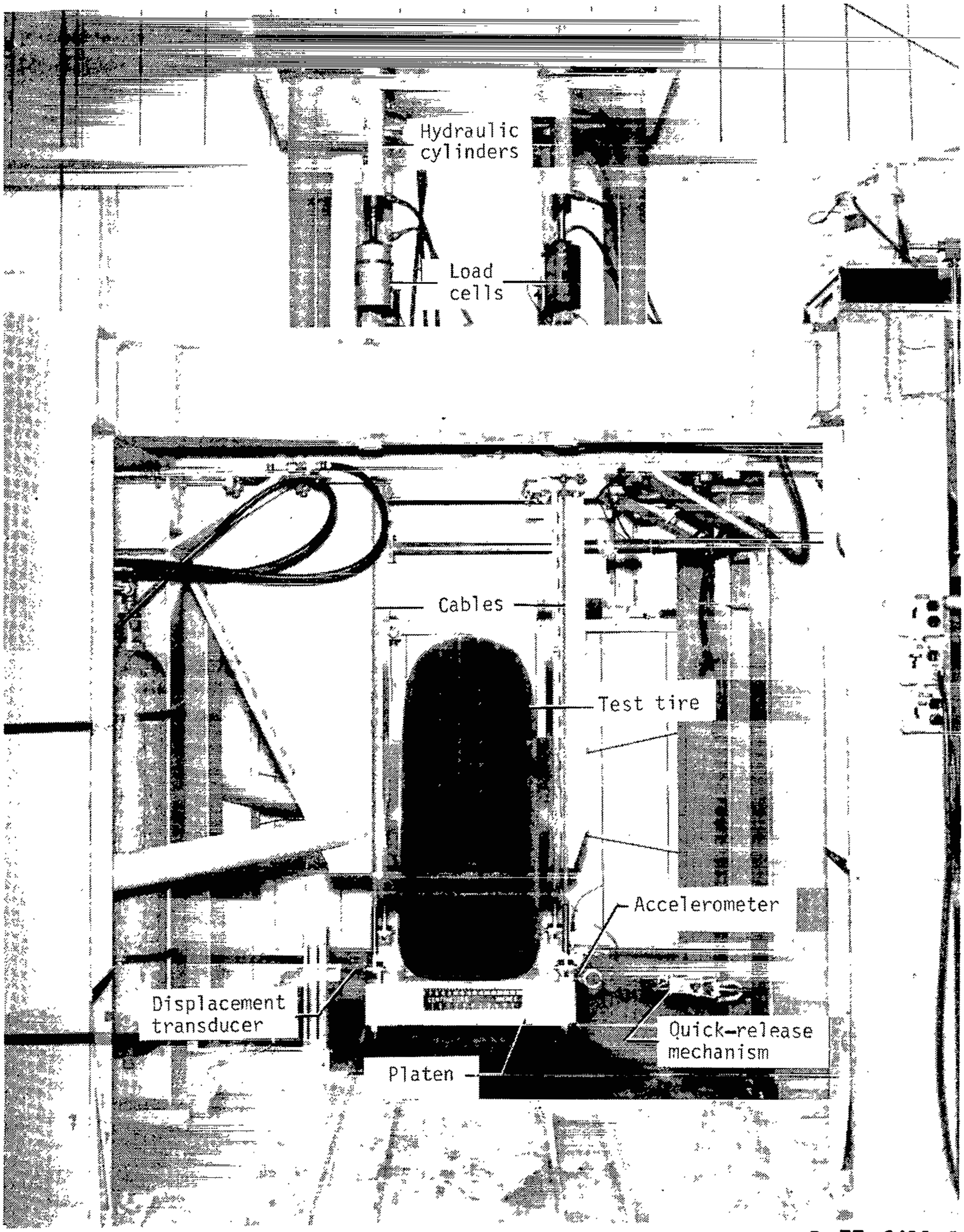

L-77-6411.1

Figure 1.- Test apparatus and test tire.

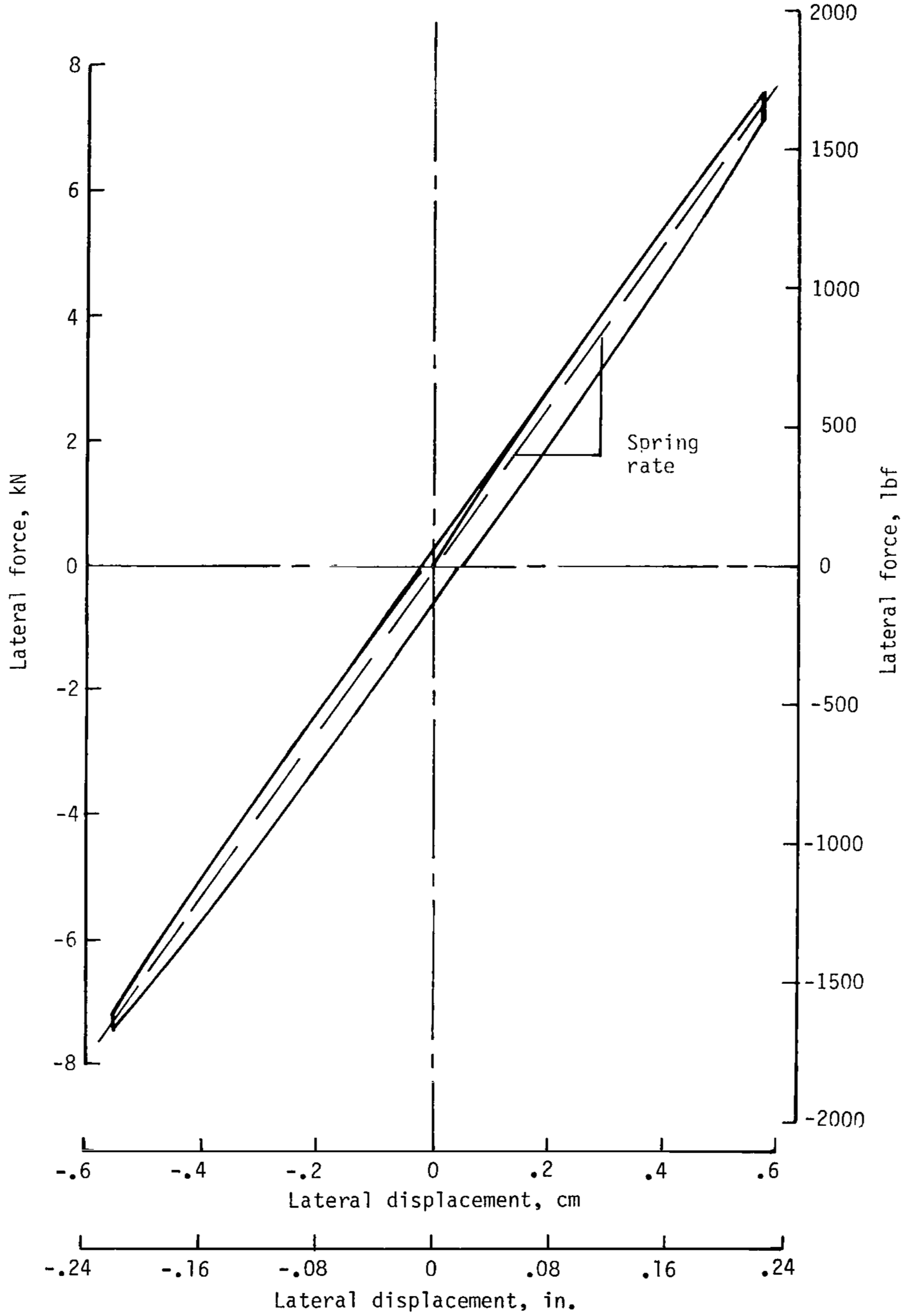

(a) Lateral direction.

Figure 2.- Typical static force-displacement curves.

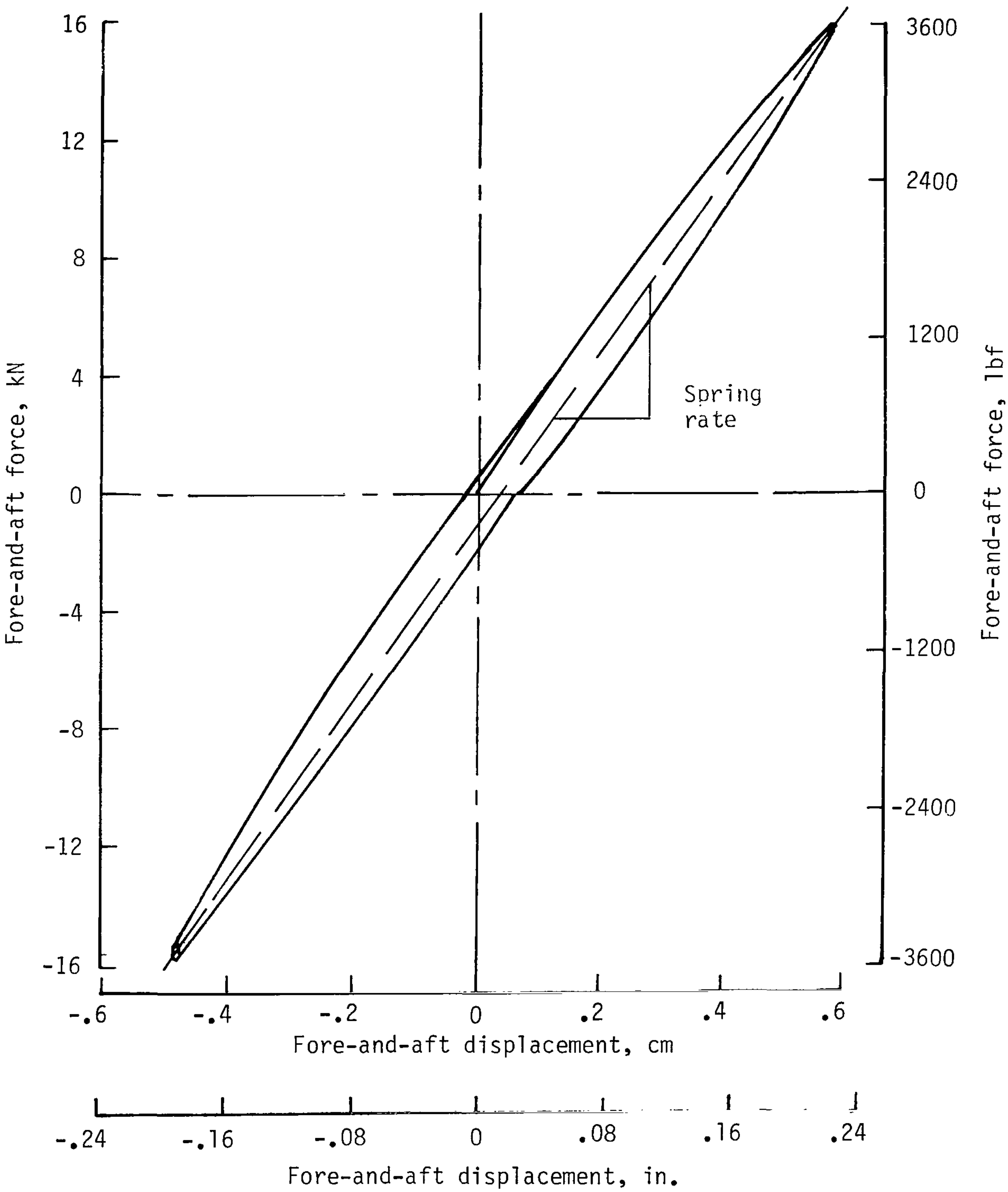

(b) Fore-and-aft direction.

Figure 2.- Concluded.

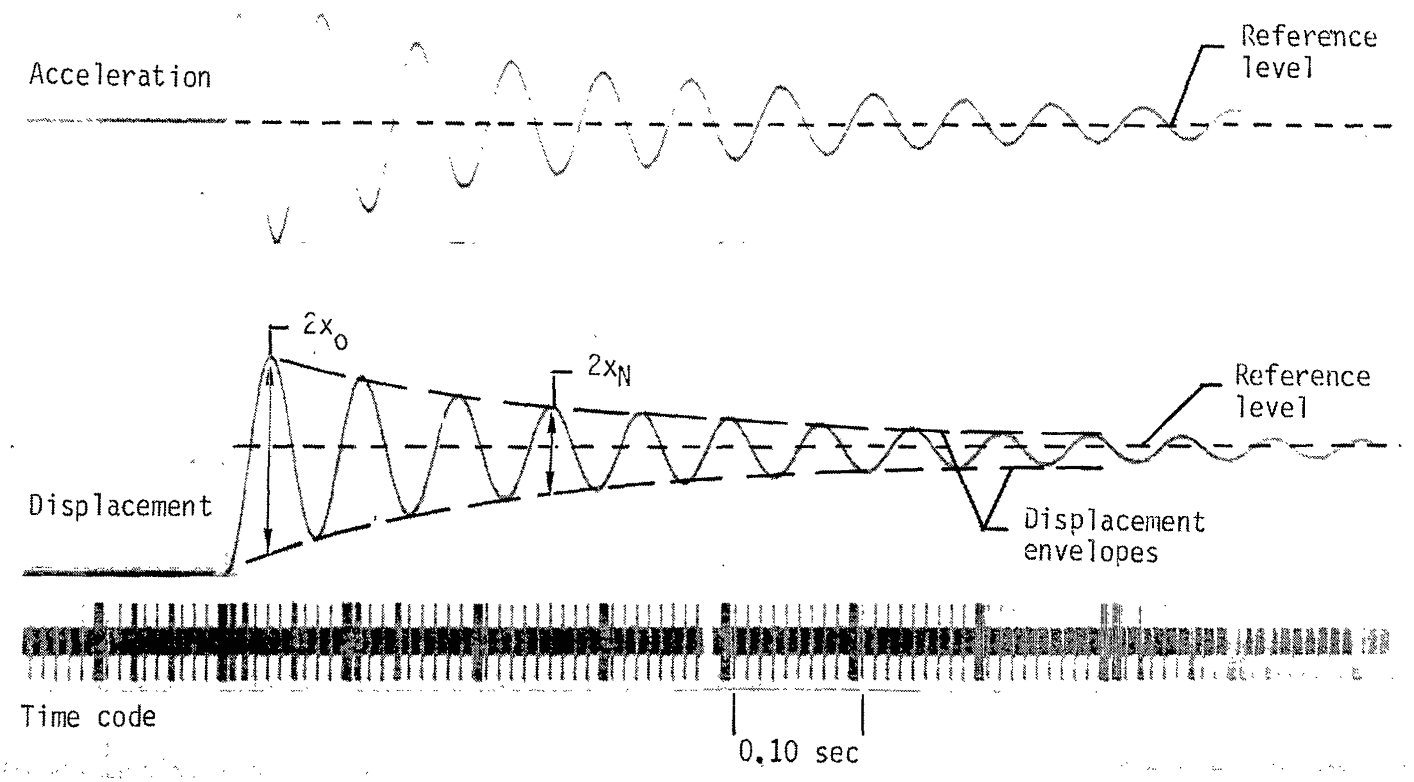

Figure 3.- Typical dynamic test time histories.

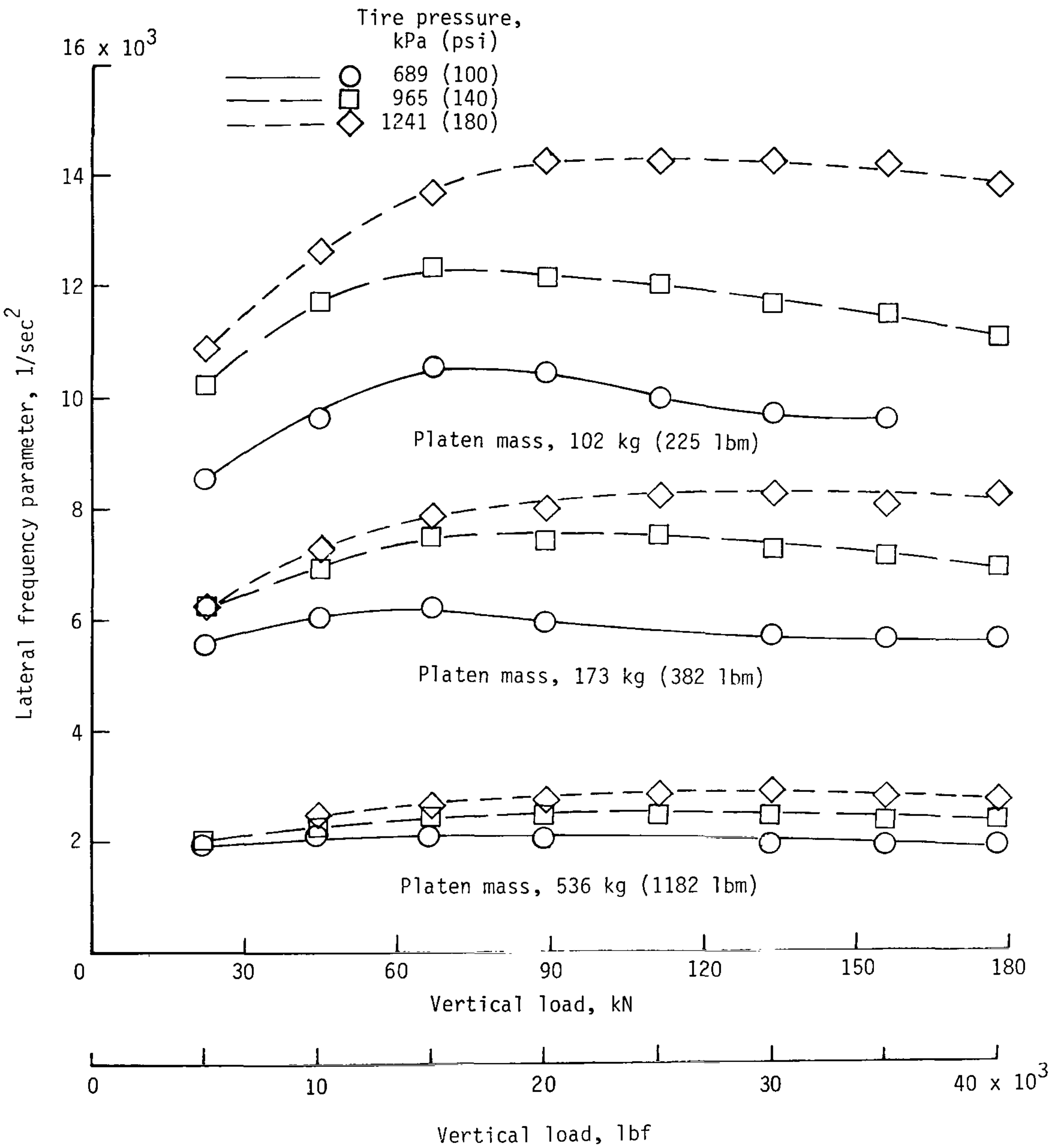

Figure 4.- Variation of lateral frequency parameter with vertical loading for three values of platen mass and tire pressure.

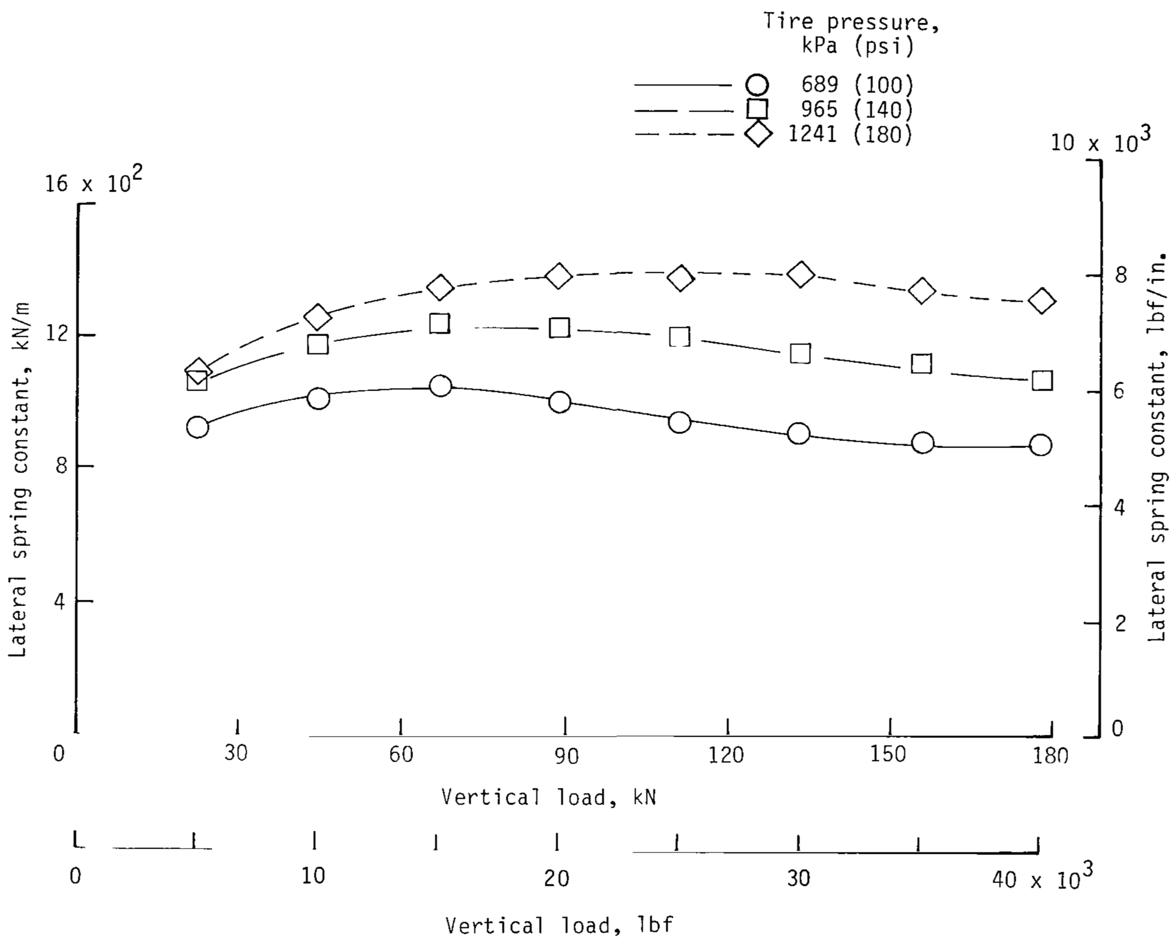

(a) Dynamic tests.

Figure 5.- Variation of lateral spring constant with tire pressure and vertical loading.

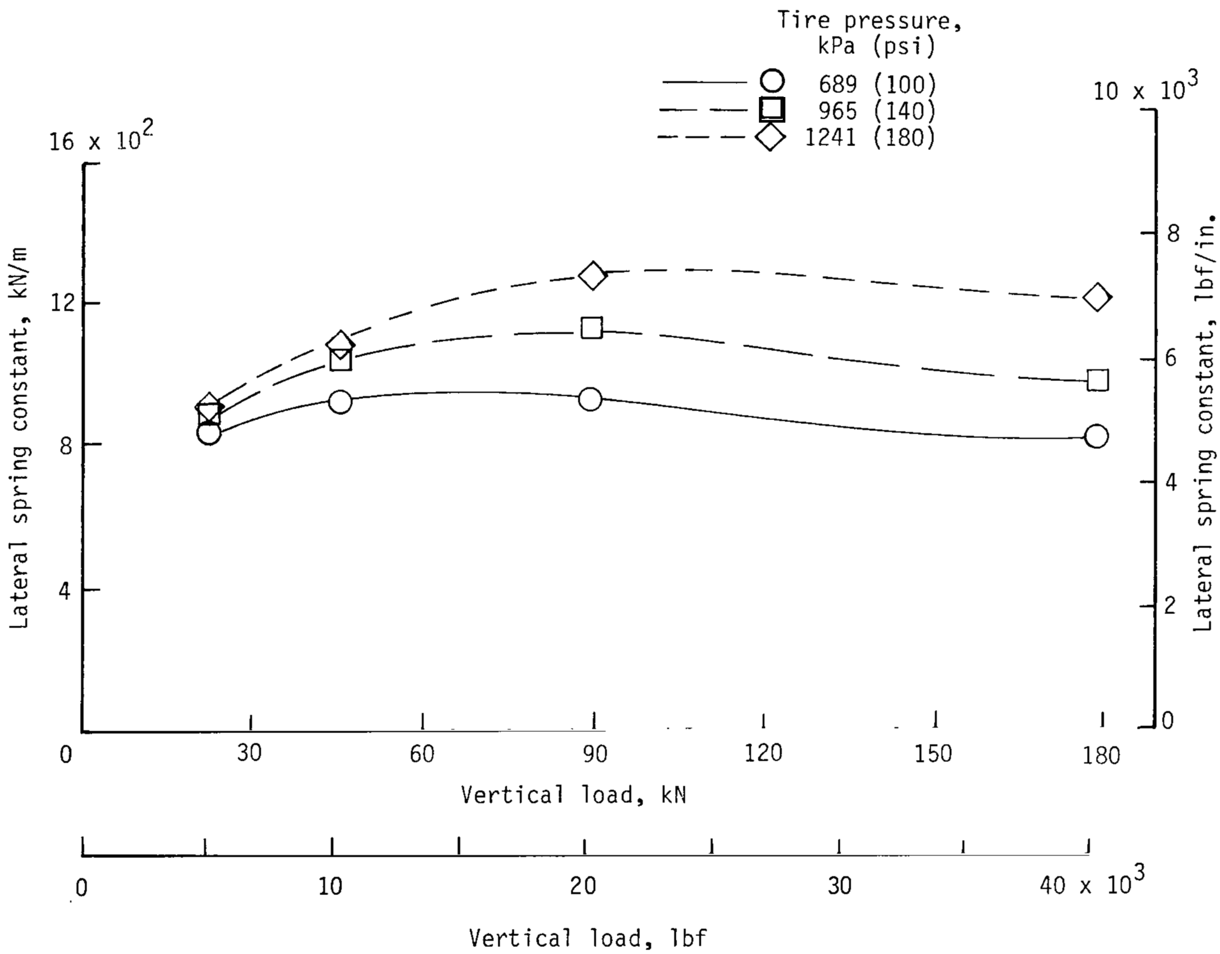

(b) Static tests.

Figure 5.- Concluded.

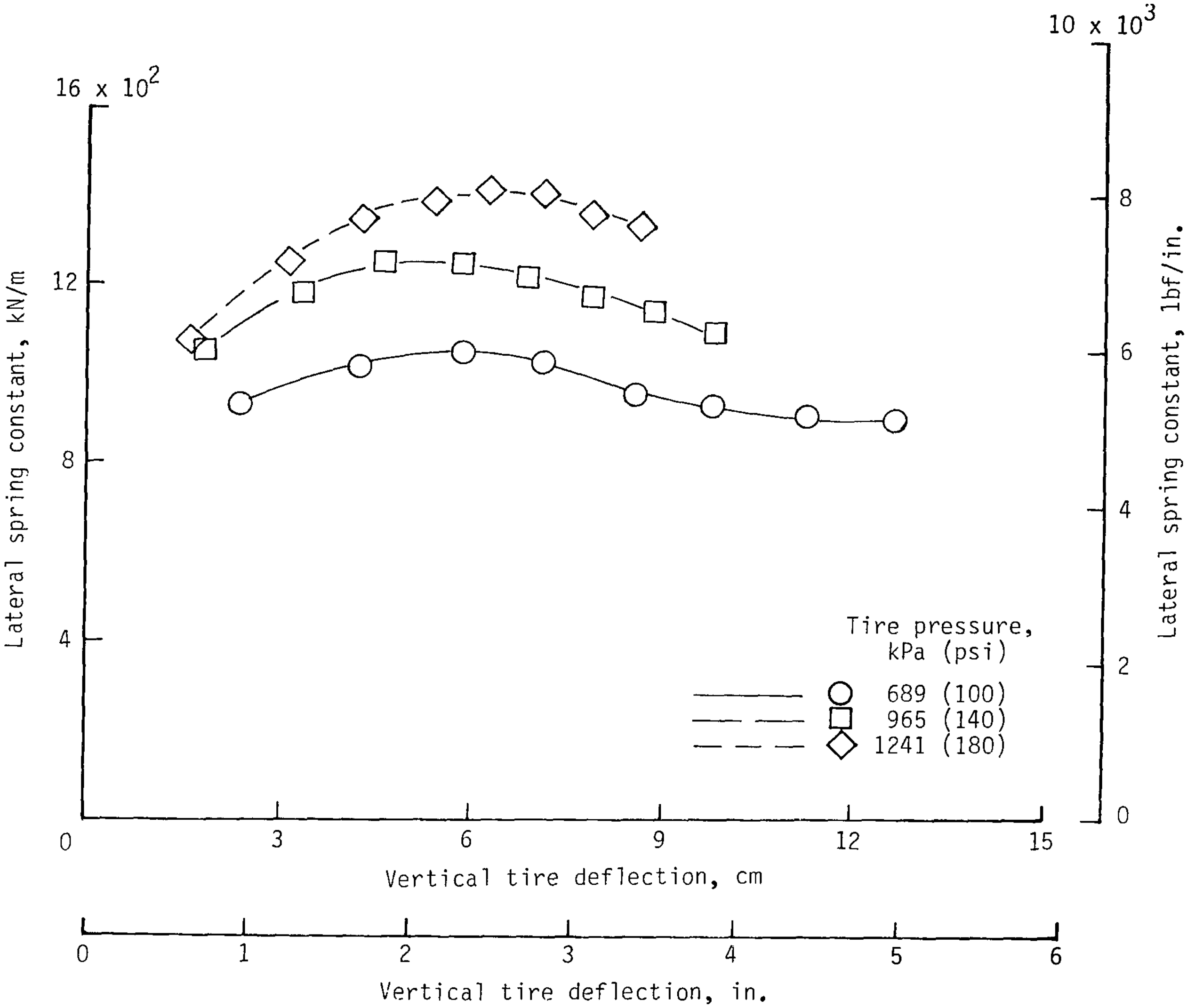

(a) Dynamic tests.

Figure 6.- Variation of lateral spring constant with tire pressure and vertical tire deflection. Spring constant values averaged from dynamic tests using three platen masses.

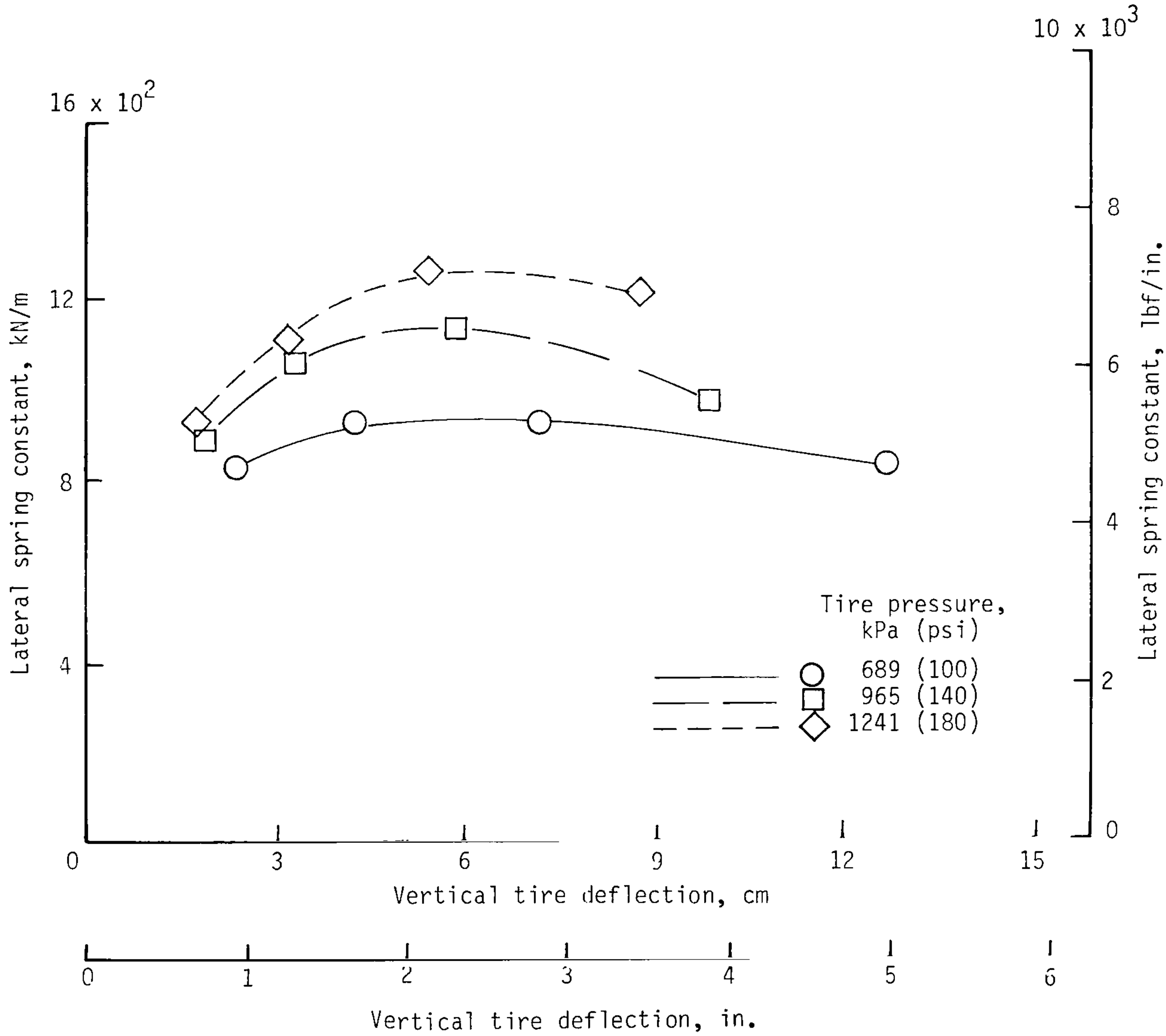

(b) Static tests.

Figure 6.- Concluded.

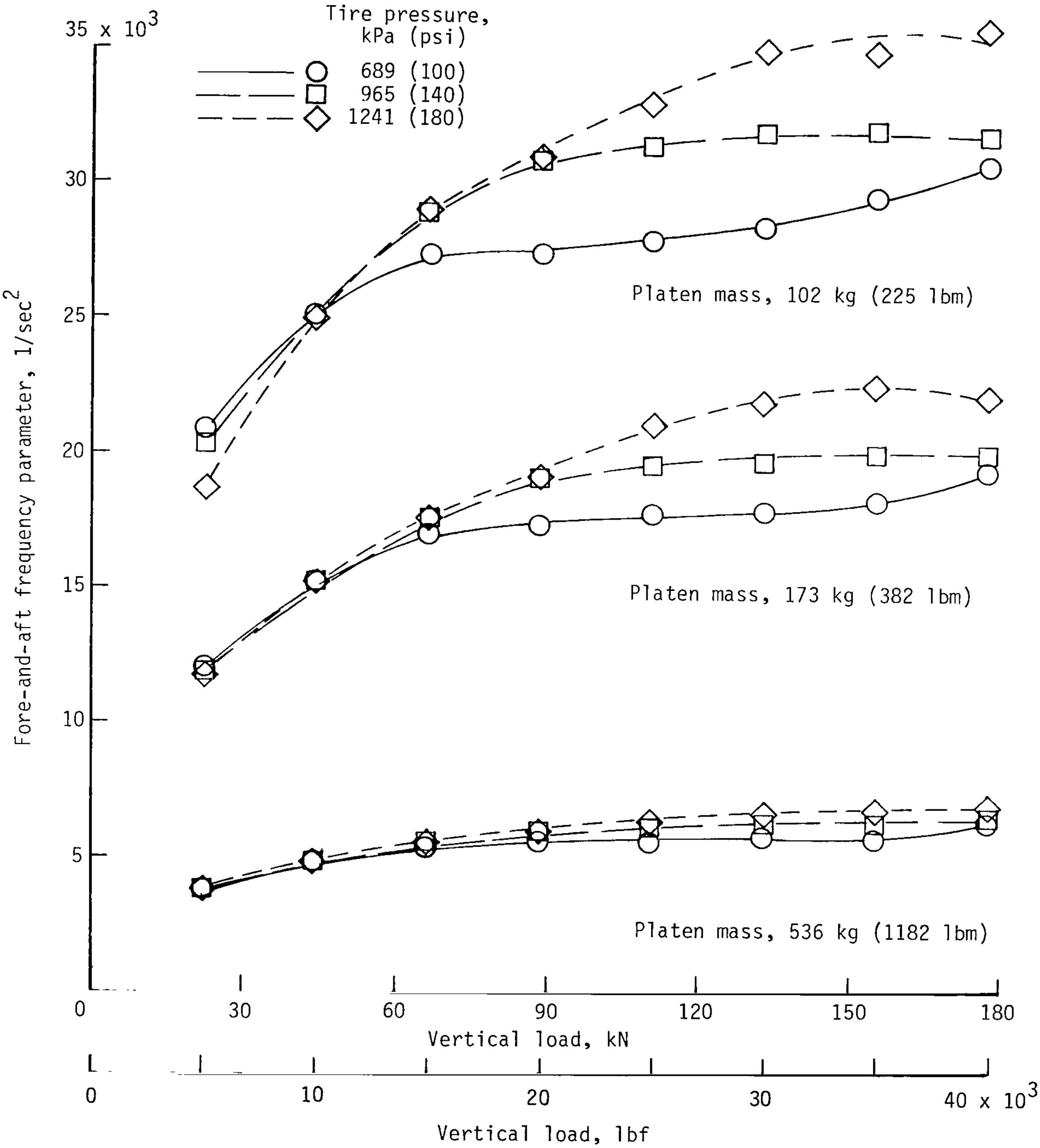

Figure 7.- Variation of fore-and-aft frequency parameter with vertical loading for three values of platen mass and tire pressure.

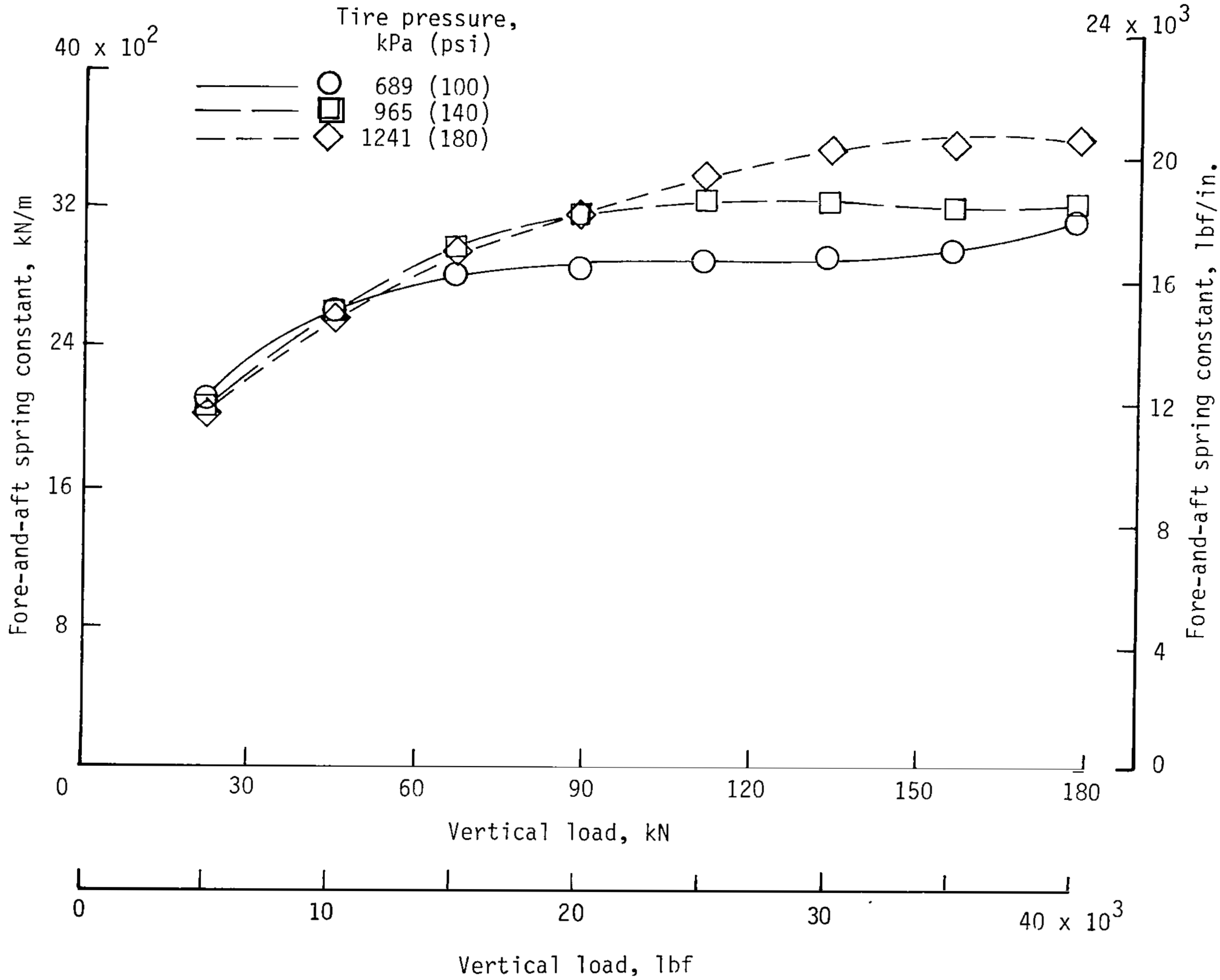

(a) Dynamic tests. Spring constant values averaged from tests using three platen masses.

Figure 8.- Variation of fore-and-aft spring constant with tire pressure and vertical loading.

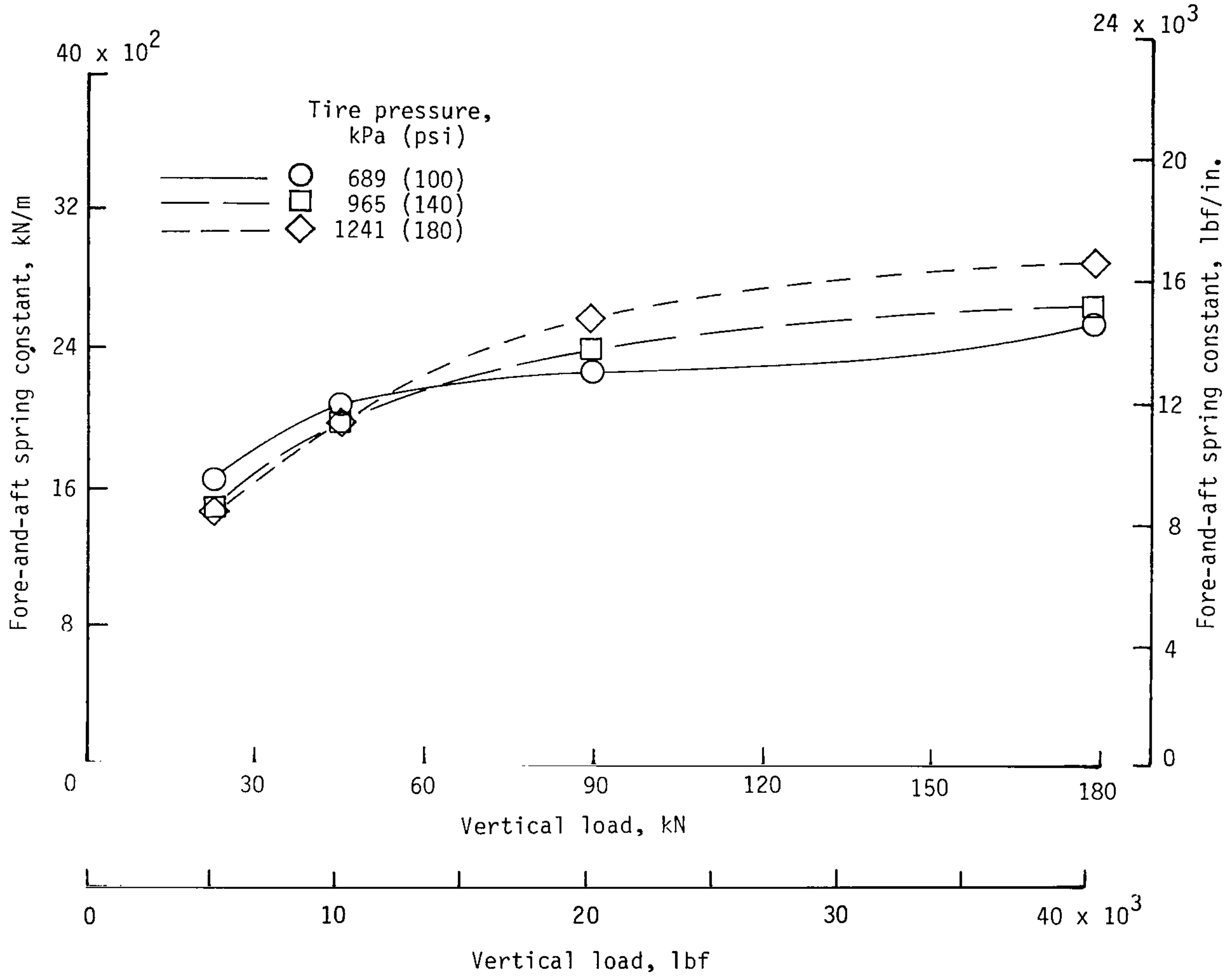

(b) Static tests.

Figure 8.- Concluded.

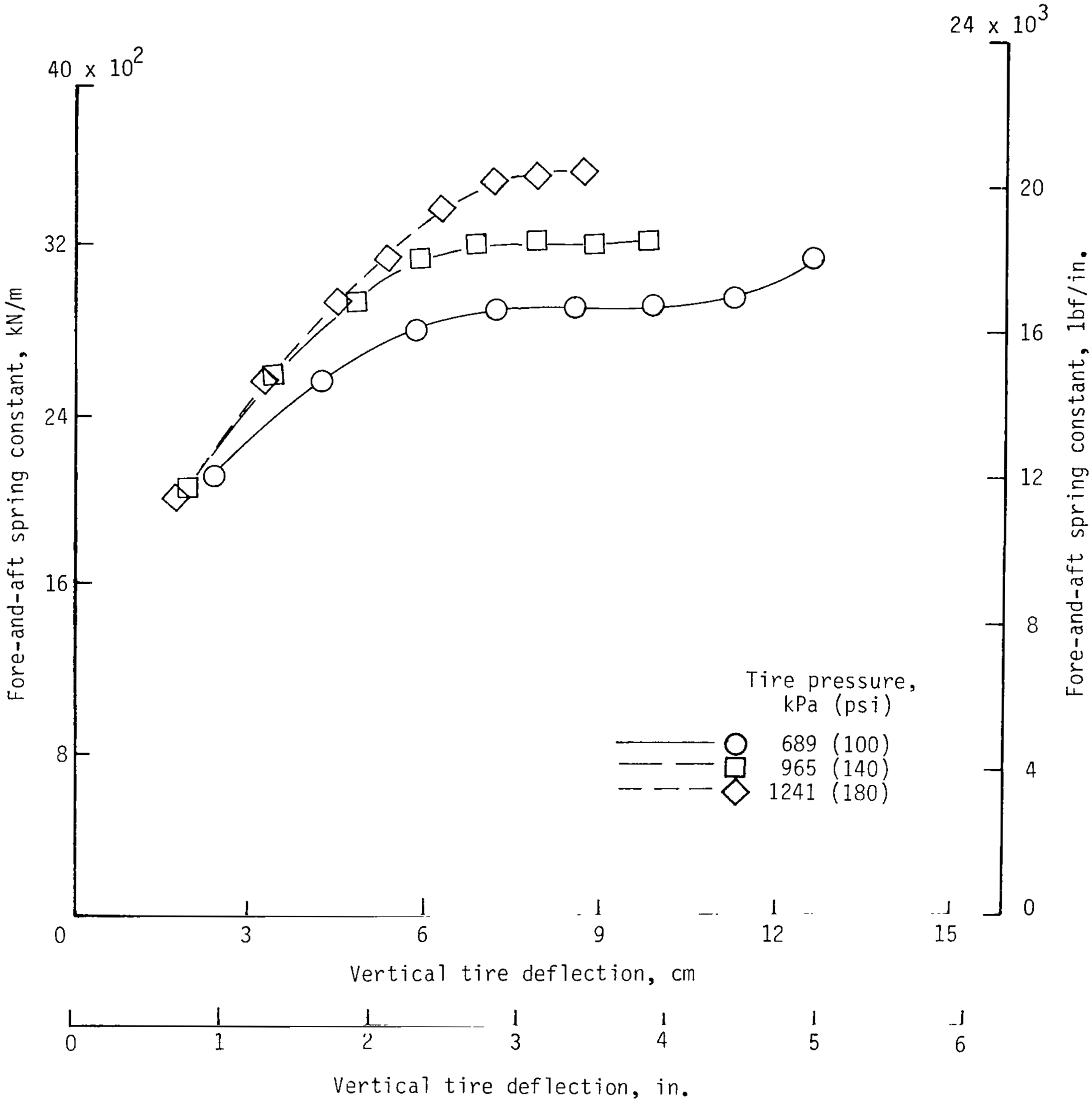

(a) Dynamic tests.

Figure 9.- Variation of fore-and-aft spring constant with tire pressure and vertical tire deflection. Spring constant values averaged from dynamic tests using three platen masses.

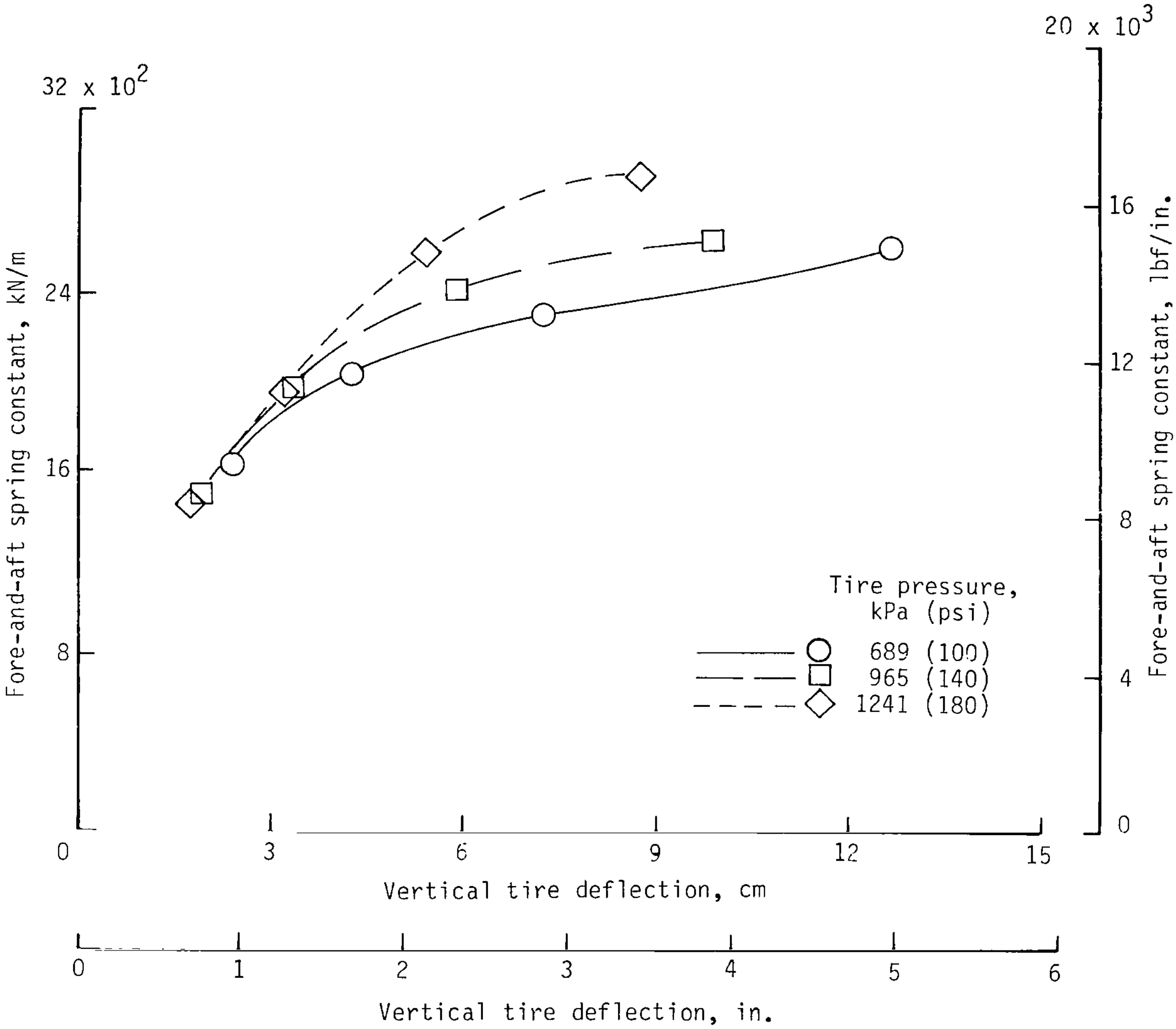

(b) Static tests.

Figure 9.- Concluded.

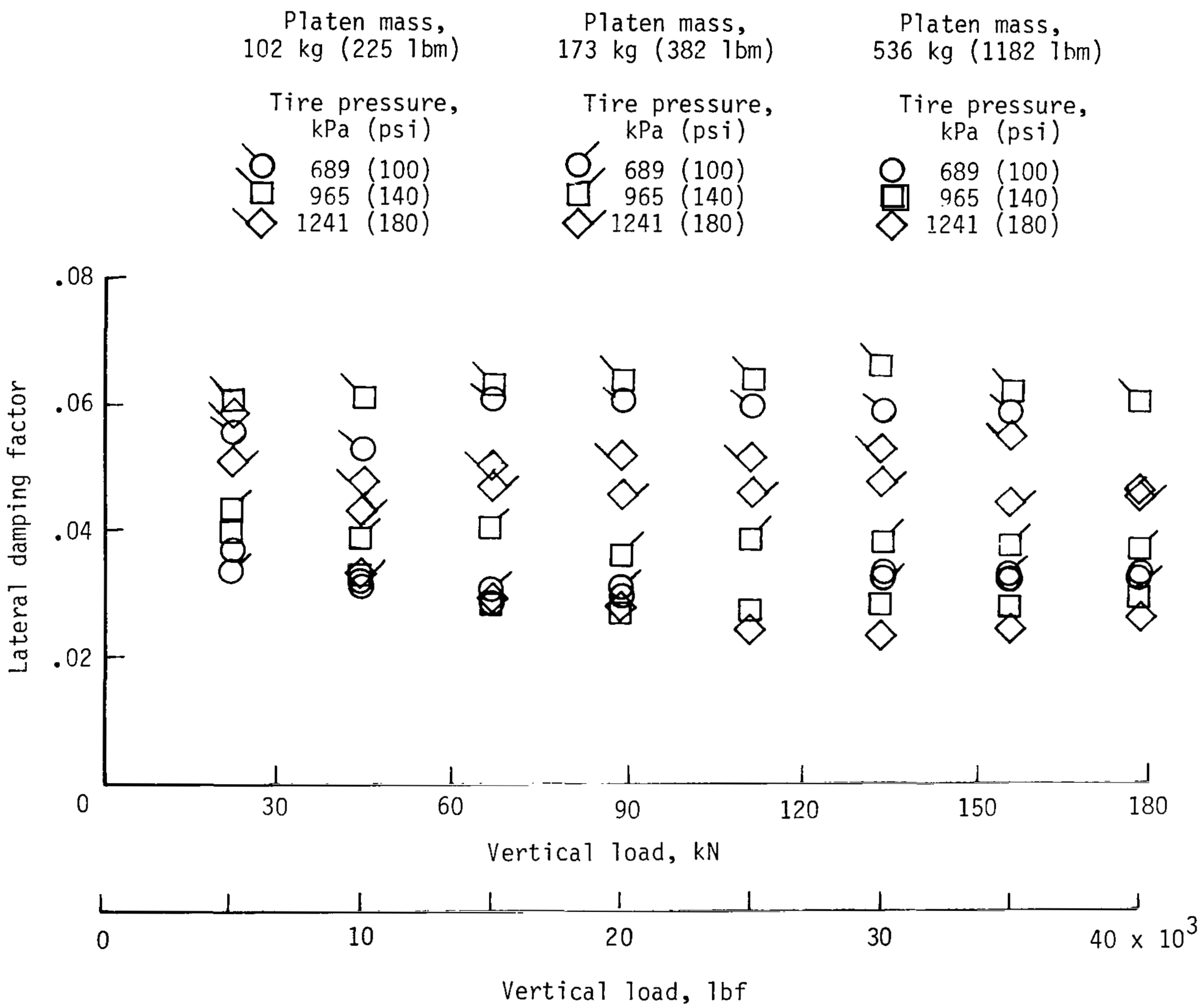

(a) Dynamic tests.

Figure 10.- Variation of lateral damping factor with platen mass, tire pressure, and vertical loading.

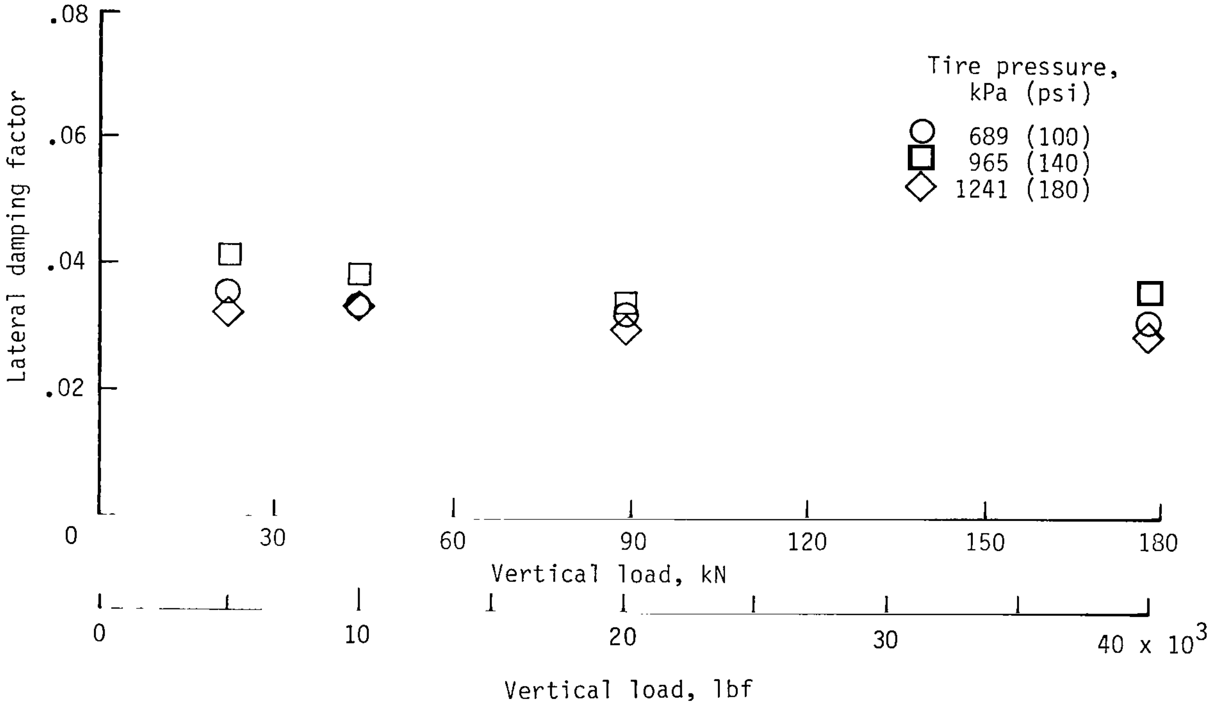

(b) Static tests.

Figure 10.- Concluded.

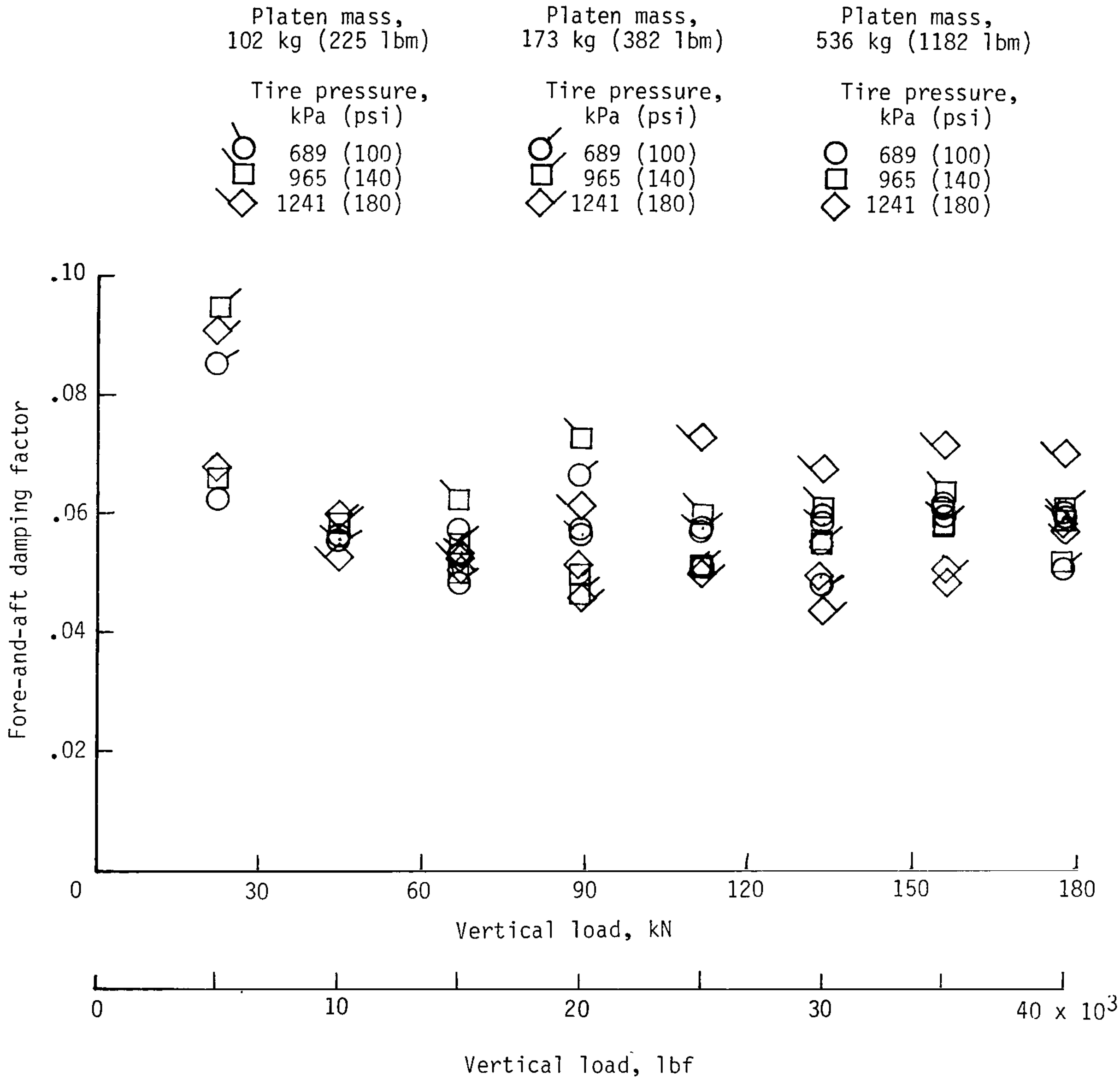

(a) Dynamic tests.

Figure 11.- Variation of fore-and-aft damping factor with platen mass, tire pressure, and vertical loading.

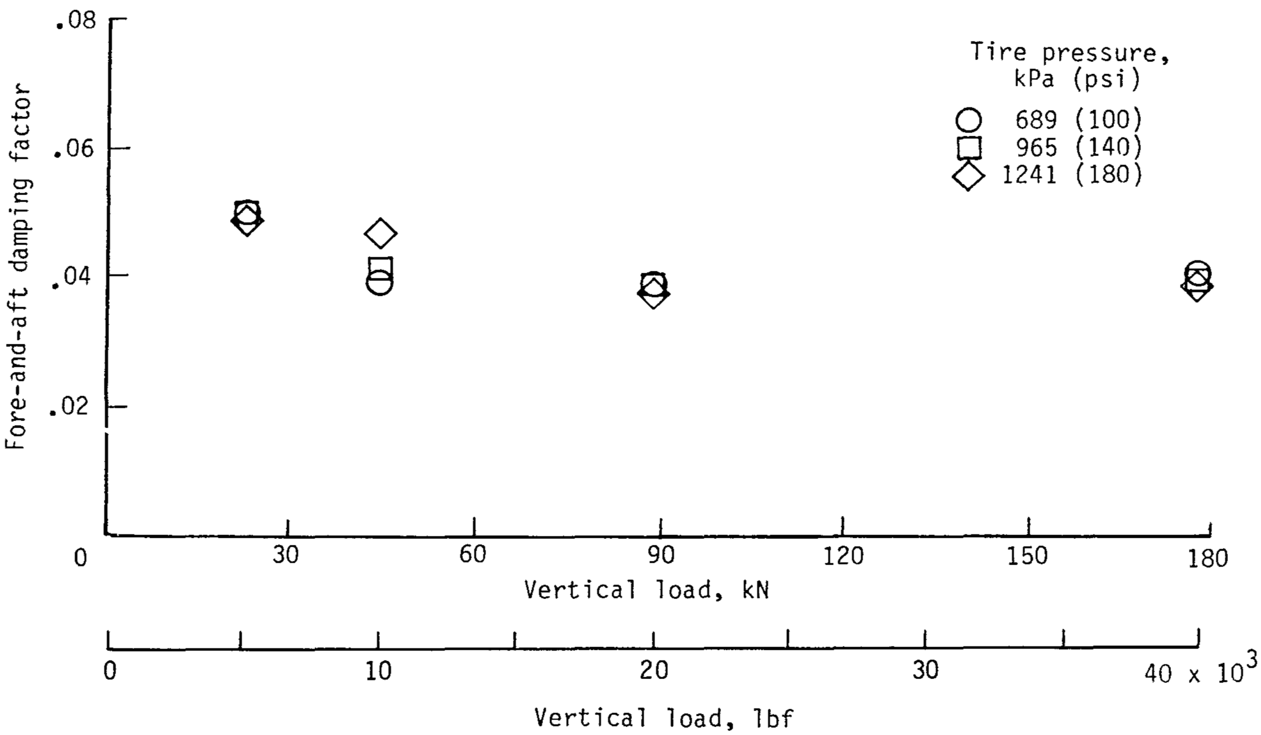

(b) Static tests.

Figure 11.- Concluded.

1. Report No. NASA TP-1671	2. Government Accession No.	3. Recipient's Catalog No.
4. Title and Subtitle TIRE STIFFNESS AND DAMPING DETERMINED FROM STATIC AND FREE-VIBRATION TESTS		5. Report Date July 1980
		6. Performing Organization Code
7. Author(s) Robert K. Sleeper and Robert C. Dreher		8. Performing Organization Report No. L-13500
		10. Work Unit No. 505-44-33-01
9. Performing Organization Name and Address NASA Langley Research Center Hampton, VA 23665		11. Contract or Grant No.
		13. Type of Report and Period Covered Technical Paper
12. Sponsoring Agency Name and Address National Aeronautics and Space Administration Washington, DC 20546		14. Sponsoring Agency Code
15. Supplementary Notes		

16. Abstract

Stiffness and damping of a nonrolling tire are determined experimentally from both static force-displacement relations and the free-vibration behavior of a cable-suspended platen pressed against the tire periphery. Lateral and fore-and-aft spring constants and damping factors of a 49 × 17 size aircraft tire for different tire pressures and vertical loads are measured assuming a rate-independent damping form. In addition, a technique is applied for estimating the magnitude of the tire mass which participates in the vibratory motion of the dynamic tests. Results show that both the lateral and fore-and-aft spring constants generally increase with tire pressure but only the latter increased significantly with vertical tire loading. The fore-and-aft spring constants were greater than those in the lateral direction. The static-spring-constant variations were similar to the dynamic variations but exhibited lower magnitudes. Damping was small and insensitive to tire loading. Furthermore, static damping accounted for a significant portion of that found dynamically. Effective tire masses were also small.

17. Key Words (Suggested by Author(s))	18. Distribution Statement
Tires Tire vibration Tire damping Tire spring constant	Unclassified - Unlimited Subject Category 03

19. Security Classif. (of this report)	20. Security Classif. (of this page)	21. No. of Pages	22. Price*
Unclassified	Unclassified	43	A03

*For sale by the National Technical Information Service, Springfield, Virginia 22161

NASA-Langley, 1980

National Aeronautics and
Space Administration

Washington, D.C.
20546

Official Business
Penalty for Private Use, $300

THIRD-CLASS BULK RATE

Postage and Fees Paid
National Aeronautics and
Space Administration
NASA-451

U.S.MAIL

5 1 1U,A, 062080 S00903DS
DEPT OF THE AIR FORCE
AF WEAPONS LABORATORY
ATTN: TECHNICAL LIBRARY (SUL)
KIRTLAND AFB NM 87117

NASA

POSTMASTER: If Undeliverable (Section 158
Postal Manual) Do Not Return